This is the final author copy of the peer reviewed accepted version of the following article: Brighenti S, Tolotti M, Bruno MC, Engel M, Wharton G, Cerasino L, Mair V, and Bertoldi W (accepted 13.6.19) *After the peak water: the increasing influence of rock glaciers on Alpine river systems* which has been published in final form at DOI:10.1002/hyp.13533. This article may be used for non-commercial purposes in accordance with Wiley Terms and Conditions for Self-Archiving.

After the peak water: the increasing influence of rock glaciers on Alpine river systems

STEFANO BRIGHENTI[1,2,4 *], MONICA TOLOTTI[2], MARIA CRISTINA BRUNO[2], MICHAEL ENGEL[3], GERALDENE WHARTON[4], LEONARDO CERASINO[2], VOLKMAR MAIR[5], WALTER BERTOLDI[1]

[1] *Department of Civil, Environmental and Mechanical Engineering, University of Trento, Trento, Italy*

[2] *Department of Sustainable Agro-ecosystems and Bioresources, Research and Innovation Centre, Fondazione Edmund Mach (FEM), San Michele all'Adige (TN), Italy*

[3] *Faculty of Science and Technology, Free University of Bozen, Bolzano, Italy*

[4] *School of Geography, Queen Mary University of London, London, United Kingdom*

[5] *Autonomous Province of Bolzano/Bozen, Office for Geology and building materials testing, Bolzano, Italy*

*Corresponding Author: Stefano Brighenti, Department of Civil, Environmental and Mechanical Engineering, University of Trento. Via Mesiano, 77 - 38123 Trento, Italy. +39 3474806941. stefano.brighenti@unitn.it

Running title: Alpine streams under increasing influence of rock glaciers

Data Availability Statement. The data that support the findings of this study are provided as Supplementary material and are available from the corresponding author upon reasonable request.

Acknowledgments. This research was carried out within the Erasmus Mundus Doctorate Program SMART (http://www.riverscience.eu) funded by the Education, Audiovisual and Culture Executive Agency (EACEA) of the European Commission. The authors thank Thomas Holtz, Federica Bressan, Federica Rotta, Domiziana Cristini, Emilio Politti, Matilde Welber, Matteo Facchini, Livia Serrao, Stefano Andrissi, Olivia West for their precious help during the field activities and longitudinal surveys, and Werner Tirler and Giulio Voto (Ecoresearch S.r.l.) for conducting the trace element analysis. The comments from two anonymous reviewers helped to greatly improve the manuscript. The authors declare no conflict of interest.

ABSTRACT

Human-accelerated climate change is quickly leading to glacier-free mountains, with consequences for the ecology and hydrology of alpine river systems. Water origin (i.e. glacier, snowmelt, precipitation, groundwater) is a key control on multiple facets of alpine stream ecosystems, since it drives the physico-chemical template of the habitat in which ecological communities reside and interact, and ecosystem processes occur. Accordingly, distinct alpine stream types and associated communities have been identified. However, unlike streams fed by glaciers (i.e. kryal), groundwater (i.e. krenal), and snowmelt-precipitation (i.e. rhithral), those fed by rock glaciers are still poorly documented. We characterized the physical and chemical features of these streams and investigated the influence of rock glaciers on the habitat template of alpine river networks. We analysed two subcatchments in a deglaciating area of the Central European Alps, where rock glacier-fed, groundwater-fed, and glacier-fed streams are all present. We monitored the spatial, seasonal, and diel variability of physical conditions (i.e. water temperature, turbidity, channel stability, discharge) and chemical variables (electrical conductivity, major ions and trace element concentrations) during the snowmelt, glacier ablation, and flow recession periods of two consecutive years. We observed distinct physical and chemical conditions and seasonal responses for the different stream types. Rock glacial streams were characterized by very low and constant water temperatures, stable channels, clear waters, and high concentrations of ions and trace elements that increased as summer progressed. Furthermore, one rock glacier strongly influenced the habitat template of downstream waters due to high solute export, especially in late summer under increased permafrost thaw. Given their unique set of environmental conditions, we suggest that streams fed by thawing rock glaciers are distinct river habitats that differ from those normally classified for alpine streams. Rock glaciers may become increasingly important in shaping the hydroecology of alpine river systems under continued deglaciation.

KEYWORDS

Hydroecology, glacier retreat, permafrost thaw, climate change, European Alps

INTRODUCTION

Current human-accelerated climate change is leading to a rapid loss of cryosphere globally (IPCC, 2013; Huss et al., 2017). In the European Alps, 76-97% of the present glacier volume is predicted to vanish within this century (Beniston et al., 2018), and the majority of glaciers to disappear within a

few decades, as most of them are very small (<0.5 km^2; Huss and Fischer, 2016). Several Alpine catchments have already surpassed the hydrological tipping point of maximum average discharge associated with glacier wastage, in relation to summer and total annual flows (Huss and Hock, 2018). After this "peak water", on the long-term discharge declines and seasonal maxima shift to the snowmelt peak of early summer (Beniston et al., 2018). The rapid glacier recession in alpine catchments is paralleled by an increased hydrological role of stochastic precipitation (Milner, Brown and Hannah, 2009; Milner et al., 2017), and by an increased prevalence of paraglacial features (i.e. adjustments in the landscape following glacier loss) and periglacial (i.e. conditioned by frost) processes driven by a slower and prolonged permafrost ice thaw (Haeberli, Schaub and Huggel, 2016). Rock glaciers are common and evident forms of mountain permafrost (Jones, Harrison, Anderson and Whalley, 2019), and their internal ice represents an important water reservoir globally (Jones, Harrison, Anderson and Betts, 2018).

Water origin is a key control of alpine stream ecosystems since it influences the habitat template (i.e. the combination of different physical and chemical conditions) in which biotic communities reside and interact along the river continuum (Hannah et al., 2007; Milner et al., 2009). Accordingly, different alpine stream types have been originally described (Ward, 1994): kryal (glacier-fed), krenal (groundwater-fed), and rhithral (snowmelt/rainwater fed). In the lower part of the catchments, the term "glacio-rhithral" is commonly used to reflect the contribution from different water sources (Füreder, 1999). Outflows from rock glaciers are commonly observed in the Alps as in other mountain ranges (Jones et al., 2019). However, to date no research has focused on characterizing the distinctive habitat template of such running waters (Brighenti et al., 2019). Rock glacier-fed (hereafter referred to as "rock glacial") streams exhibit particular hydrological and chemical conditions, comprising cold (<1.5°C) and clear waters with high electrical conductivity associated with high concentrations of major ions and, often, trace elements (Thies, Nickus, Tolotti, Tessadri and Krainer, 2013; Colombo et al., 2018a; Rotta et al., 2018a). Solute concentrations typically increase from spring to autumn, when the baseflow can be sustained by thawing internal ice (see Colombo et al., 2018a). Due to their cold waters, rock glacial streams were found to decrease summer water temperature in tributaries along the river continuum, thus extending refuge areas for cold-adapted species (Harrington, Hayashi and Kurylyk, 2017). In general, rock glaciers (including fossil forms, i.e. those without ice) and other landscape features including talus bodies, moraines, and tills represent important groundwater sources (Clow et al., 2003; Wagner, Pauritsch and Winkler, 2016; Winkler et al., 2016; Rogger et al., 2017; Harrington, Mozil, Hayashi

and Bentley, 2018) that are able to influence the quantity and quality of running waters in alpine catchments (Liu, Williams and Caine, 2004; Weekes, Torgersen, Montgomery, Woodward and Bolton, 2015; Engel et al., 2019). However, most research to date has focused on the hydrology of single landforms (e.g. for talus bodies see Muir, Hayashi and McClymont, 2011; for moraines Winkler et al., 2016; for rock glaciers Harrington et al., 2018; Winkler et al., 2016), and we are not aware of any study attempting a longitudinal characterisation of stream conditions under their combined influence at the catchment scale. In fact, glaciers are generally considered as the major hydroecological driver during the snow-free season in glacierized catchments (e.g. Ilg and Castella, 2006; Brown, Milner and Hannah, 2010).

Our research therefore aimed to characterize the habitat features of rock glacial streams and appraise the seasonal and diurnal patterns of glacial, periglacial, and paraglacial influence along glacier-fed streams. We tested two hypotheses: H1) Rock glacier outflows represent a distinct alpine stream type, with different physical and chemical conditions when compared to kryal, krenal and glacio-rhithral habitats; H2) Rock glaciers influence stream conditions along the river continuum, in catchments with small glacier cover and fading glacial influence. We investigated the physical and chemical characteristics of different stream types within a glacierized catchment, and characterized the influence of glaciers, permafrost, mountain landforms, and groundwater on the stream habitat conditions moving downstream from the glacier snout.

STUDY AREA

The Solda Valley (Figure 1A) is located in the Central Italian Alps, in the Ortles/Cevedale massif. The climate is typically alpine, with average temperatures ranging from 10.6 °C in July to -5.3 °C in January and an average annual precipitation of 860 mm (Autonomous Province of Bolzano/Bozen – APB, 2018a) at Solda village (1900 m a.s.l., 1982/2012 period). The research was conducted in the upper Solda and Zay subcatchments, which both have their closing section in Solda village. The area hosts several glaciers (World Glacier Monitoring Service - WGMS, 2018) and active rock glaciers occurring above ~2700 m a.s.l. (APB, 2018b). Three tectonic units of the Austroalpine domaine (Ortles, Zebrù and Peio) merge in the valley resulting in a complex geology (Montrasio et al., 2015). To reduce this bedrock variability, we selected the study sites (Table 1, Figure 1B) within the crystalline basement (Campo Nappe), mainly composed of gneisses and quartzphyllytes.

The upper Solda subcatchment (area 20 km^2, maximum elevation 3902 m a.s.l.) hosts several glaciers covering 32% of the total area (APB, 2018b). Among these, the North-oriented Suldenferner (1.05 km^2, mean elevation 2986 m a.s.l.) is a debris-free glacier that has experienced considerable retreat during the last decades (320 m during 1920-2016 period; WGMS, 2018). Sampling sites (Figure 1B) included the stream originating from this glacier (S1, S2), the permanent outflow (SRG) of an active rock glacier (area 0.072 km^2) located in the alpine belt, and one of the several springs originating from the slopes in the subalpine belt (i.e. SKN, Table 1).

The smaller Zay subcatchment (11 km^2, 3546 m a.s.l., Figure 1C) is geologically more homogeneous (gneisses, with some intrusions of amphibolites in the lower section). Three small glaciers (area <0.5 km^2) cover 8 % of the subcatchment area. Among them, the North-oriented Ausserer Zay (0.3 km^2) is a debris-covered glacier that retreated 260 m from 1897 to 2007 (WGMS, 2018), and additional 90 m from 2008 to present (comparison between the present front and the 2008 orthophoto of the APB, 2018). The main stream of the subcatchment (Zay Stream) originates from this glacier (station Z1), whereas no other major surface runoff originates from the other glaciers (Figure 1C). The Zay Stream has a complex flow path (Figure 1C, Table 1): 400 m below the glacier snout (Z3), the stream feeds a small lake (0.044 km^2, 2772 m a.s.l.) whose outflow immediately sinks into moraine debris. The moraine outflow (Z4), located 200 m downstream, runs beside the body of an active rock glacier (0.09 km^2, 2719 m a.s.l. front), and joins with its outflow (ZRG, Table 1) in a small glacial floodplain (Z5, Table 1). Downstream, the closing section (Z6) of the glacial cirque (5.2 km^2) also drains a series of three proglacial lakes without any evident outlet, and a huge rock glacier (0.42 km^2) that feeds a very small spring not directly connected with the Zay Stream. Beyond the glacial cirque, the stream seeps into the debris of a talus slope, from which it re-emerges after a distance of 600 m and an elevation 290 m lower (Z7, Figure 1C). The slopes of this lower part of the subcatchment are occupied by some intact and several relict rock glaciers without any evident superficial outflow. In the sub-alpine belt, groundwater-fed tributaries, including the one where the ZKN station is located, join the Zay Stream before station Z12. In the lower part, the stream flows through a coniferous forest (Z13) before reaching the Solda village (Figure 1).

METHODS

Streams were investigated during two consecutive years (2017, 2018). Sites (Figure 1, Table 1) were sampled during five-day campaigns conducted in three main periods of the alpine summer:

snowmelt (3rd week of June), glacier ablation (end July/beginning of August), and flow recession (1st week of September). Several additional field-trips were undertaken during summer 2018 for discharge measurements and supplementary surveys. We designed two types of survey, differing in aims and monitored parameters: extensive surveys and longitudinal surveys.

Extensive surveys

These surveys (N=6) characterized the physical and chemical conditions of streams as a function of water origin. At each subcatchment, we selected one groundwater-, one rock glacier-, and one glacier-fed stream. Additionally, four stream sections of mixed origin were selected along the Zay Stream (Figure 1C). A total of twelve stations (reaches) of ~50 m length each were investigated.

Water temperature, electrical conductivity (EC), and turbidity were recorded with portable probes (WTW-Cond-3310 and WTW-Turb-430IR, Germany). Water level was recorded (in 2018) by measuring the water surface elevation at fixed iron rods. Discharge (not assessed at ZRG and Z5 because the very wide and shallow channels prevented complete transversal mixing) was measured with the salt-dilution method (Gordon, MacMahon and Finlayson, 1992) during periods of maximum and minimum flow, and was used to build flow-rating curves associated with water level. A gauging station equipped with a level-meter pressure transducer (Keller AG Messtechnik, Switzerland) was deployed near the Zay closing section (Z13, 2081 m a.s.l.) for continuous recording at 10 min intervals. All extensive survey stations were instrumented with temperature data-loggers (HOBO© WaterTempProv2, Onset, Germany), with 30 min interval records. Temperature datasets were used to calculate the maximum (T_{max}), minimum (T_{min}), average water temperature (T_{avg}) and temperature range ($dT= T_{max}-T_{min}$) for each survey week.

Water samples for chemical analyses were collected in 500 mL polyethylene bottles and preserved at 4°C until analysis at the Hydrochemistry laboratory of the Edmund Mach Foundation. Alkalinity, pH, EC, CO_3^-, Ca^{2+}, Mg^{2+}, Cl^-, Na^+, K^+, total nitrogen (TN), NH_4^+-N, NO_3^--N, total phosphorus (TP), PO_4^--P, $SO_4^{2-}$and SiO_2, were determined according to standard methods (APHA-AWWA-WPCF, 2017). Stream water for the determination of trace elements was filtered with cellulose acetate membranes (0.45 µm) into acid washed 100 mL polyethylene bottles and acidified at 1-1.5% with >65% HNO_3 until delivered to Ecoresearch S.r.l. laboratory (Bolzano), where concentrations of Be, B, Na, Mg, Al, K, Ca, Ti, V, Cr, Mn, Fe, Co, Ni, Cu, Zn, As, Se, Rb, Sr, Mo, Ag, Cd, Sn, Sb, Ba, Tl, Pb, U, Bi, P were measured using a ICP-MS ICAP-Q, Thermo Fischer analyser. Water samples for the determination of Dissolved Organic Carbon (DOC) were collected in clean, pre-acidified (65% HNO_3),

100 mL polyethylene bottles and preserved at 4°C until delivered to Dolomiti Energia S.p.a. laboratory (Trento).

To identify the major runoff components for each station and sampling time, precipitation, snowmelt, ice-melt and stream water samples were collected in 50 mL polyethylene bottles. A time-integrated precipitation sample was collected each month (from May to October) in rainwater containers built by following the IAEA (2014) standards, and placed nearby SRG and ZRG stations. Snowmelt and ice melt samples were taken from dripping snow patches and glacier surface rivulets at each sampling occasion. Isotopic analysis of δ^2H and $\delta^{18}O$ was conducted with a laser spectroscope (Picarro L2130i, precision: 0.1‰ for δ^2H, 0.25‰ for $\delta^{18}O$) at the laboratory of the Free University of Bozen/Bolzano.

Channel stability was assessed with the Pfankuch index (Pfankuch, 1975), obtained by recording metrics describing: upper banks (landform slope, mass-wasting, debris jam potential, vegetation, channel capacity); lower banks (rock content, obstructions, undercutting, deposition); and the streambed (rock angularity, brightness, particle packing, clasts size, scouring and deposition, aquatic vegetation). Scores assigned to each variable are summed in order to achieve the index, with low and high scores associated with stable and unstable channels, respectively. An aliquot of water (250-3000 mL) was collected and filtered in the field through GF/C Whatman glass microfiber filters, that were stored frozen (<-20°C) until the determination of suspended solids concentration, which was calculated as ash-free dry mass (AFDM, g L^{-1}) following Hauer and Lamberti (1996). The organic detritus was sampled with a Surber net (100 µm mesh, 506 cm^2 frame) by disturbing different substrates (i.e. mosses, boulders, cobbles and gravel) according to their relative abundance in the channel (five total replicates). Samples were preserved in 90% ethanol and devoid of invertebrates and fragments of living mosses under a dissecting microscope. Organic detritus was calculated as ADFM (g m^{-2}). The coarse (≥ 1 cm) and fine (< 1 cm) fractions were separated with a sieve to calculate the detritus ratio (coarse/fine).

Longitudinal surveys

These surveys (N=3) estimated the diel and seasonal variability of glacier influence on habitat conditions along the river continuum. Longitudinal surveys were conducted at the Zay subcatchment, where we selected 13 monitoring points (Figure 1D), that included all extensive survey stations and additional sites that were added to obtain a more regular spacing. Monitoring was undertaken on days without precipitation during the extensive survey campaigns of 2018. Two

teams assigned respectively to the upper (Z1-Z6) and lower (Z7-Z13) stations of the subcatchment measured water temperature, EC, turbidity and water level every three hours starting from 7 AM (five runs of approximately 60 min each), proceeding downstream (ZKN and ZRG were included). Portable conductivity (WTW-Cond-3310, WTW-Cond-3210) and turbidity (WTW-Turb-430IR) meters were previously cross-calibrated in the laboratory to ensure comparable recording between the two teams. Station Z1 was not sampled in June as it was covered with snow. Due to safety reasons (dry thunderstorm), 4 PM and 7 PM runs in lower Zay (Z7-Z13) were not undertaken in September. Six additional surveys with morning, mid-day and afternoon runs were conducted in different weeks respect to longitudinal surveys, and were included in the calculation of the glacial indices (see below). The data recorded by the gauging station at Z13 and the data-loggers were used to provide information about the discharge and temperature patterns of the period and guarantee that the longitudinal survey data were representative of each hydrological period. The Pfankuch index was assessed for all the longitudinal survey stations. Discharge measurements were conducted using the salt dilution method at Z2, Z3, Z4, Z6, Z8, Z11 during seasonal discharge minima and maxima, to evaluate the discharge range, and flow rating curves were developed.

Data analysis

To detect the different components of the water flow, mixing diagrams for each subcatchment were produced by plotting δ^2H against SiO_2 values, where silica was assumed as a proxy for groundwater contribution (Ward, Malard, Tockner and Uehlinger, 1999; Brown, Hannah and Milner, 2003; Liu et al., 2004; Brown et al., 2006). In addition, we used a tracer-based runoff separation and produced two-member mixing models. Accordingly, mass balance equations 1 and 2 were applied to separate discharge into two flow components (Blaen, Hannah, Brown and Milner, 2014):

$$Q_{gw} / Q_i = (C_m - C_i) / (C_m - C_{gw}) \quad \text{(Equation 1)}$$

$$Q_i = Q_m + Q_{gw} \quad \text{(Equation 2)}$$

where Q denotes discharge and C the solute (Silica) concentrations. Subscripts gw, m and i refer to groundwater, melt water, and sampling site water, respectively.

We assumed that meltwater was driven by the snowmelt or the ice melt (for both found below the detection limits, i.e. 0.05 mg L^{-1}). The groundwater component was defined as the highest value at

krenal sites (for both SiO_2 = 4.3 mg L^{-1}). The uncertainty was calculated following Genereux (1998) and accounting for the error propagation where data were pooled together.

The extensive survey dataset was analysed by Principal Component Analyses (PCA), with Kaiser normalization and Varimax rotation, to visualize the environmental variables associated with different stations and sampling date. Trace elements were analysed in a separate PCA from the other environmental variables, in order to account for bedrock composition variability. Stepwise forward selection, discarding the variables not strongly correlated (correlation coefficient <0.5) to any other in the correlation matrix, was used to choose the variables. Water isotopes (analysed separately), detritus ratio (redundant with organic detritus), suspended solids (redundant with turbidity), and trace elements above the detection limits for less than 6 samples were excluded from the multivariate analyses.

The longitudinal survey dataset was analysed to compute the glacier influence and its spatial and temporal trends. The Glaciality Index proposed by Ilg and Castella (2006) uses the normalized values of water temperature, EC, 1/suspended solids, and 1/Pfankuch (only bottom component) to produce a non-centred PCA, where the PC1 scores are taken as values of the index. We used a similar approach and built our Index of Glacial Influence (IGI) by using 1/water temperature, 1/EC, turbidity, and Pfankuch (upper banks, lower banks and bottom components) in order to obtain increasing IGI values associated with increasing glacial influence. The IGI values were eventually obtained by adding to PC1 scores the minimum value of them, to achieve all positive numbers. Given the large seasonality of the glacier influence in alpine catchments (e.g. Milner and Petts, 1994; Brown et al., 2003), we designed a specific index of Seasonal Glacier Influence (SGI), reflecting the large seasonal variability of habitat conditions driven by the presence of glaciers. This index was obtained using the same method employed for the calculation of the IGI by using the following variables in the PCA: Pfankuch index; total averages of turbidity; 1/water temperature; 1/EC; and the standard deviation values of turbidity and EC. We cross-compared (non-parametric Spearman correlation, ρ) our calculated indices with the total area occupied by glaciers in the underlain catchment area (Glacier cover in the catchment) and the Glacial Influence index of Jacobsen and Dangles (2012), calculated as a function of distance from the glacier and its area.

Ggplot2 package in R version 3.6.0 (R Development Core Team, 2017) was used to produce biplots of mean and standard deviation of the variables across the gradients over the season. Pairwise comparisons (Table 2) were made to analyse differences in all the analysed variables between sample groups (i.e. months, stream types). Due to non-normal distribution (Shapiro-Wilk,

P<0.5), even after data transformation, and/or inhomogeneous variances (Levene, P>0.5), we used the non-parametric Wilcoxon rank-sum and the Kruskal-Wallis tests, with post-hoc Mann-Whitney test and Bonferroni corrections. The softwares SPSS (v.25, IBM, 2018) and R were used to analyse the data.

RESULTS

Discharge patterns, water origin and temperature profiles

The hydrograph at Zay gauging station (Figure 2) revealed major peaks during the snowmelt period (first week of June in 2017, last week of May in 2018). In both years, discharge decreased during summer, especially after early September, with superimposed secondary peaks associated with rainfall events in July and August (Figure 2). Discharge decreased consistently from the snowmelt to recession period along the whole Zay stream (Figure 3), including the proglacial sites (Z2-Z3), where it was 55 ± 10 L s^{-1} in June, 35 ± 17 L s^{-1} in August, and 13 ± 10 L s^{-1} in September (longitudinal surveys means and standard deviations). Discharge at the Suldenferner snout (S1; all extensive survey measurements always at 10-11 AM), exhibited a different trend, with the highest values recorded in August (136 L s^{-1}), intermediate values in June (113 L s^{-1}), and much lower values in September (12 L s^{-1}) surveys.

Seasonal variations of both $\delta^{18}O$ and $\delta^{2}H$ revealed a significant isotopic enrichment from June to September (Table 2), in line with a decreased influence from the melting snow. This seasonality is shown in the mixing space of $\delta^{2}H$ and SiO_2 (Figure 4), where all stream samples are included in the range of the potential water sources for both subcatchments. With very low silica concentrations (<0.3 mg L^{-1}), snowmelt (-140.3 to -89.7 ‰) and ice melt (-105.5 to -89.5 ‰) delineate an end-member of isotopic depleted waters, and precipitation a second end-member of isotopically enriched (-91.2 to -38.8 ‰) waters. Sampling station waters were in the isotopic range of snowmelt and ice melt, and differed in terms of silica concentrations, with lowest values for the upper kryal (0.6 ± 0.4 mg L^{-1}) and highest for krenal sites (3.7 ± 0.8 mg L^{-1}) at each extensive survey. Rock glacial, lower kryal, and glacio-rhithral sites exhibited similar silica concentrations at each extensive survey, intermediate between kryal and krenal. Accordingly, the mixing models (Table 3) revealed for all periods an increased groundwater contribution from the upper kryal sites (14.1 ± 9.9 % overall mean and SD), to the lower kryal (44.4 ± 10.8 %) and glacio-rhithral (48.3 ± 13.0 %) stations, and to the krenal sites (84.9 ± 19.6 %). Rock glacial streams revealed a high proportion of

groundwater contribution (49.2 ± 12.7 %), without any significant difference between ZRG and SRG (Table 3).

Temperature data-loggers showed different patterns according to stream type (Figure 5). Low water temperature with reduced diel fluctutations characterized the Zay glacier outlet (Z1, T= 0.7 ± 0.5°C), where diel fluctuations increased in mid summer, but remained limited when compared to downstream stations. Marked diel fluctuations characterized Z3, where water temperature (T= 2.1 ± 1.2°C) even exceeded 8°C during warm days after the snowmelt (with up to 8°C fluctations). Moving downstream, the outlets from the moraine (Z3, T= 2.5 ± 0.5°C) and the talus body (Z7, T= 4.7 ± 0.8°C) exhibited increasingly high average temperatures but less pronounced diel fluctuations, compared to Z3. The krenal station ZKN showed constant and relatively low water temperature in summer (T= 3.1 ± 0.3°C), with slight diel fluctuations of maximum 1°C. Rock glacial streams exhibited unique patterns (Figure 5), with low water temperatures slightly increasing over the season, and almost absent diel fluctuations (1.2 ± 0.1°C for both ZRG and SRG). The temperature profile of SRG exhibited more pronounced daily fluctuations than ZRG, and showed transient (0.5-1.5 hrs) peaks (up to 2.6°C) associated with rainfall events. Also the upper kryal station showed transient temperature peaks, apparently associated with rainfall events, although these fluctuations were less frequent and minor (not shown).

Extensive surveys

The first two components of the PCA with the retained environmental variables (Figure 6) explained 72.6% of the total variance, and the variable loadings are summarized in Table 4. Samples were clearly separated according to stream type and seasonality. Upper kryal stations could be distinguished in terms of their low PC1 and PC2 values. Accordingly, pairwise comparisons (Table 2) showed that upper kryal stations had significantly higher Pfankuch index (i.e. channel instability), suspended solids, turbidity, and total P, and lower SiO_2, organic detritus, and detritus ratio compared to the other stream types. However, in September, the upper kryal stations exhibited significantly lower turbidity values and higher EC, NO_3^-, SO_4^{2-}, Ca^{2+}, than in June and August (Table 2), and the strong seasonal variability of the habitat conditions was also identified in the PCA by a progressive shift towards positive values of PC1 and PC2 (Figure 6). Samples from upper kryal to lower kryal, glacio-rhithral, and krenal stations were distributed along a gradient of decreasing water turbidity and

increasing channel stability, water temperature and abundance of organic detritus (Figure 6, Supplementary A). In fact, a strong negative correlation (ρ=-0.84, P<0.001) was identified between PC1 values and the Jacobsen Index of glaciality in the catchment. Within each stream type, the PC values shifted from June to September along a gradient of increasing solute concentrations (Figure 6, Supplementary II). Nevertheless, this variability was minimal for krenal stations (confirmed by non-significant differences among the three periods in the variables). At each sampling occasion krenal stations exhibited the highest values of SiO_2, organic detritus, and detritus ratio among stations, although differences in mean values were significant only when compared to upper kryal stations (Table 2). Rock glacial streams exhibited significantly lower T_{max} and dT compared to all other stream types, and the lowest T_{avg} except for those of kryal stations. However, only SRG can be clearly distinguished in Figure 6, due to the particularly high values of PC1 , while ZRG scores are placed in the same range of lower kryal stations except for September values, that are associated with increased PC1 scores. In fact, the two rock glacial streams exhibited clear differences in water chemistry, with SRG showed significantly higher pH, EC, Ca^{2+}, Mg^{2+}, SO_4^2, HCO_3^-, K^+, Pfankuch index values, and lower turbidity and total nitrogen than ZRG (Table 2). In both rock glacial streams, NO_3^- levels (108-272 $\mu g\ L^{-1}$) were comparable to those of glacio-rhithral and lower kryal in all samples, and showed highest values in September, while PO_4^- concentrations (1-5 $\mu g\ L^{-1}$) were among the highest of all stream types in all periods (see Supplementary A for further details).

In the PCA undertaken with the retained trace elements (As, Sr, Ba, Al, Rb and U), 74.7 % of the variance was explained by the first two components (Figure 7, Table 4). One outlier (Z3, September 2017) was removed before running the analysis because of extremely high concentrations of Al and Fe (see Discussion). All June samples except SRG plot close to the PCA axes origin, due to low concentrations of trace elements. At the krenal sites, trace element concentrations remained for the whole season close or below the detection limits (see Supplementary B). For the other stream types, August and September samples are spread along the two PC axes in Figure 7, and clearly differ in the two subcatchments, with upper kryal and rock glacial samples from Solda grouped along PC1 (increasing As, Sr, Ba) and Zay samples grouped along PC2 (increasing Al, Rb, U). The pairwise comparisons (Table 2) confirmed this pattern (higher values of Rb and U and lower values of Ba and Sr at Zay), and provided further detail on the distinction between habitats based on the trace elements discarded in the PCA. In fact, upper kryal exibited significantly higher values of Mn (up to 22.3 $\mu g\ L^{-1}$) compared to all other stream types. The highest trace elements concentrations were detected in September at both Zay (U, Mn and in 2017 Fe, Al,

Rb) and Solda (As, Sr, U, and Ba, Ni, Cu, Rb only in this month) upper kryal (Supplementary B). U exhibited high concentrations along the entire Zay stream over this period, with higher values in the proglacial sections (68.1-88.3 μg L^{-1}) than downstream (6.6-35.7 μg L^{-1}). High concentrations of trace elements were also detected in rock glacial waters, in particular SRG that showed the highest concentrations of As (22-36 μg L^{-1}), Sr (29.5-614 μg L^{-1}) and Ba (11.8-24 μg L^{-1}) among stations in all periods (Figure 7, Supplementary B). In September, concentrations of U at ZRG (53.2-81.9 μg L^{-1}) were comparable to those of Zay upper kryal, and higher than those of the nearby lower kryal sites (6.6-35.7 μg L^{-1}).

Longitudinal Surveys

The first component of the PCA used to build the Index of Glacial Influence explained 59.1% of the total variance (see Table 5 for the loadings). In the PCA run to build the Seasonal Glacier Influence (SGI), the first component alone accounted for 79.4% of the variance and was strongly driven by all the parameters included in the analysis (Table 5). Both IGI and SGI were significantly correlated ($P<0.001$) with distance from the glacier and elevation (correlation coefficient $\rho=-0.80$ for IGI, $\rho=-0.98$ for SGI), Jacobsen Index ($\rho=0.8$; $\rho= 0.98$), and the glacier cover in the catchment ($\rho=0.66$; $\rho=0.85$). Longitudinal patterns were similar for both IGI and SGI (Figure 8) exhibiting significantly higher values (Table 2) in the proglacial reaches (Z1-Z3) compared to further downstream (Z4-Z13), with a sharp reduction from station Z4, i.e. downstream of the lake and the moraine. Longitudinal variations of both indices were stronger in the proglacial reaches than below the lake, reflecting a rapid reduction of the glacial influence moving downstream from the glacier snout on a daily (IGI) and seasonal (SGI) basis. IGI exhibited a clear seasonality, with lowest values during the flow recession compared to both snowmelt and glacier ablation periods. These longitudinal and temporal patterns of the indices corresponded closely to those of channel stability, water temperature, EC, turbidity, and discharge recorded along the stream.

The Pfankuch index had the same longitudinal trend as the IGI, with relatively high values recorded at the floodplain station (Z5), driven by high values of the bottom component, and below station Z10, driven by high values of the upper and lower bank components (Figure 9). The index showed a strong negative correlation with distance from the glacier ($P<0.001$, $\rho= -0.80$).

All stations above the proglacial lake (Z1-Z3) showed significantly higher turbidity and lower water temperature and EC compared to the stations downstream (Z4 to Z13) in all periods (Figure

10). These proglacial reaches showed a clear seasonality, with the recession period characterized by significantly lower discharge, and higher EC compared to the periods of snowmelt and glacier ablation (which did not differ significantly from each other in relation to these parameters).

Below the lake (Z4 to Z13), the Zay stream showed sudden shifts in terms of decreased turbidity (up to 6-fold) and increased EC (3-fold) during snowmelt and glacier ablation, compared to proglacial stations, and decreased water temperature compared to Z3. Moving downstream from the moraine outlet, EC increased slightly during snowmelt and glacier ablation, especially in the lower part of the subcatchment (below Z10), and showed a positive peak below the junction with the rock glacial stream (Z5). This peak was particularly pronounced (228.8 ± 8.0 µS cm^{-1}) and sharp during the recession period, with a rapid decrease in EC just below this station. The seasonal increase of EC was also found at ZRG (Figure 10), with highest values during recession (295.9 ± 7.6 µS cm^{-1}, 4-fold increase with respect to the previous periods), corresponding to the highest levels recorded at Zay. At ZRG, the longitudinal surveys confirmed seasonally low and constant water temperature (1.2 ± 0.1°C), while turbidity (8.3 ± 5.2 NTU) values were always comparable to those recorded below the talus body. ZKN was characterized by consistently clear (1.2 ± 1.1 NTU) and cold (3.2 ± 0.3°C) waters in all longitudinal surveys, and EC showed a small seasonality (130.0 ± 7.1 µS cm^{-1}) as well, with higher values compared to all other stations (including ZRG) during snowmelt and glacier ablation but not during recession, when EC was higher (not significantly) than at stations Z10-Z13 and Z1-Z4.

Different patterns of diel fluctuations appeared to be associated with different seasonal phases (Figure 11), although it was not always possible to disentangle the timing of minima and maxima in the parameters, and the values recorded from stations downstream of the moraine (especially Z4 and Z7-Z13) showed very little diel variability (Figure 10). Water temperature generally showed morning minima (in all periods) and mid-day (in the recession period) to afternoon (in the snowmelt and glacier ablation periods) maxima. These timings were confirmed by the analysis of the temperature data-loggers (which recorded, for the proglacial stations as well, the actual minima during the night, when in-situ field measurements could not be undertaken). Turbidity showed a comparable diel pattern across all periods in the proglacial reaches (Z1-Z3), with afternoon maxima and morning minima. A clear opposite trend was observed in the lower part of the subcatchment (Z7-Z13) during glacier ablation, where maxima were recorded in the early morning and minima in the late afternoon. A spatial pattern in EC values was observed during glacier ablation, when all the upper stations showed morning maxima (except Z4) and afternoon

minima (except Z4 and Z6), while the lower stations (Z7/Z13) had morning minima and afternoon maxima. Discharge values showed similar patterns for all stations and across all periods, with morning minima and afternoon maxima where variations could be detected. Finally, IGI diel cycles appeared to be most strongly related to the trends recorded for turbidity, with a weaker contribution from the other parameters structuring the index (Figure 11).

DISCUSSION

This study combined field sampling, to characterize the physical and chemical water quality and habitat parameters of alpine streams, with high-frequency monitoring to investigate the longitudinal gradients of glacial influence in different periods of the Alpine summer. Using this combined survey design we addressed both research hypotheses: i) we identified key habitat features that distinguish rock glacial streams from other stream types (H1) and ii) we demonstrated the role of an active rock glacier in shaping the stream habitat conditions along the river continuum, in a catchment where the hydrological imprint of glaciers is fading because of the prolonged retreat and the influence from the paraglacial landscape is increasing (H2).

Discharge and water sources

Discharge patterns suggest a greater hydrological role of the glacier in Solda than in Zay. In fact, the discharge at the Suldenferner outflow was an order of magnitude higher than at the Ausserer Zay glacier, with major peaks during the period of glacier ablation. In contrast, discharge maxima at the upper kryal stations (and along the entire stream) at Zay occurred in the early summer, i.e. during the snowmelt period. This seasonal dynamic, combined with the extreme reduction of the glacier during the last few years (WGMS, 2018), provides evidence that the Zay subcatchment was well over the peak water. In fact, a similar condition was observed for small glaciers in Switzerland (Huss and Fischer, 2016), where anticipation of the seasonal peak discharge and decreased average discharge were observed in 1961-1990 following glacier retreat, and were associated with the exceedance of peak water. At the catchment scale, the reduced hydrological contribution from predictable glacier cycles is paralleled by an increased relative importance of melting snow and a larger dependency on stochastic precipitation patterns, as reported for several catchments in the Alps and the Pyrenees (Milner et al., 2017).

At Zay, the progressive groundwater contribution in the lower sections suggested by mixing models is in line with previous studies in alpine settings, where silica was found to be a good indicator of groundwater (Ward, Malard, Tockner and Uehlinger, 1999; Brown et al., 2003; Liu et al., 2004; Brown et al., 2006). However, the isotopic composition of water (assessed during baseflow conditions) indicates that at least part of the groundwater flow in Zay was associated with the routing of glacial- and snow melt waters. This meltwater contribution to groundwater recharge was also demonstrated by Ward et al. (1999) in a highly glacierized catchment, and our results suggest that glaciers are still able to provide a notable contribution to water fluxes even in catchments with a small glacier cover.

Stream types

Despite the differences in the hydrochemistry of the two studied subcatchments reflecting the prevalence of different bedrock, our study has provided further evidence that water origin is a key driver in structuring habitat conditions in alpine streams (e.g. see Ward, 1994; Brown et al., 2003). The upper kryal stations were characterised by the harshest and most variable habitat conditions among all surveyed stations. In fact, highly unstable channels with very turbid and cold waters, enriched in total phosphorus (product of the glacial physical erosion; see Hodson, 2007) and depleted in other solutes, were typical of the snowmelt and glacier ablation periods. Shifts to clear waters with a steady flow occurred in September, when a 10-fold increase in EC was detected compared to August. Multiple energy fluxes (e.g. net radiation and sensible heat) influence the ablation process on glaciers (Hannah, Gurnell and McGregor, 2000), and ice ablation is reduced or absent during autumn and winter (Cuffey and Paterson, 2010). Accordingly, autumn discharge from glaciers is typically dominated by the baseflow (see Table 3), which is mostly driven by the subglacial/englacial contribution associated with waters enriched in solutes (Sharp, 2006) and metals/metalloids (Mitchell, Brown and Fuge, 2001). Accordingly, highest concentrations of major ions (Ca^{2+}, Mg^{2+}, SO_4^{2-}, NO_3^-) and trace elements were recorded in this period in both glacier-fed streams. Interestingly, As (S2), U (the entire Zay Stream), Fe and Al (Z3, 2017) were found above the EU/EPA limits for drinking water in September, likely as a result of the local lithology and the presence of metal ores in the upper Zay (siderite at manganese; Baumgarten, Folie and Stedingk, 1998).

As previously reported for highly (e.g. Milner and Petts, 1994; Füreder, 2012; Finn, Räsänen and Robinson, 2010) and poorly (e.g. Smith, Hannah, Gurnell and Petts, 2001; Khamis, Brown,

Hannah and Milner, 2016) glacierized basins, a gradient of habitat amelioration was detected along the glacier-fed stream. This steep gradient we observed was associated with decreasing turbidity and trace element concentrations, and increasing channel stability, average water temperature, nitrate concentrations, and abundance of organic detritus, the latter due to higher inputs from the surrounding vegetation and increased retention from bryophyte mats.

Water temperature represents the main environmental variable that discriminates rock glacial streams from the other habitats, as very low (<1.2°C) and constant values were recorded at both rock glacial streams . Carturan et al. (2016) suggested a low and constant temperature during summer as the only reliable water proxy allowing identification of the permafrost presence in rock glaciers. However, the studied rock glacial streams were also characterized by clear waters, with an abundance of organic detritus that was comparable to glacio-rhithral stations. Despite the scarce loads from the surrounding vegetation (patchy alpine grassland), this indicates a higher retention capacity of rock glacial compared to kryal habitats, which is also due to the higher coverage of mosses and higher channel stability. Nutrient levels, i.e. nitrates and phosphates, were also high and comparable to those of glacio-rhithral sections, and potentially support primary production (Uehlinger, Robinson, Hieber and Zah, 2010). High nitrate levels are commonly found in rock glacier outflows and have been attributed to microbial production into the rock glacier bodies, where the ice thaw may promote the nitrogen flushing from microbially active sediments (Williams, Knauf, Cory, Caine and Liu, 2007; Baron, Schmidt and Hartman, 2009; Barnes, Williams, Parman, Hill and Caine, 2014).

Although it was not possible to clearly discriminate rock glacial streams according to water isotopes, these streams exhibited concentrations of silica comparable to those of lower kryal and glacio-rhithral stations in all periods, suggesting a considerable part of the baseflow associated with the groundwater component. This is in line with the literature on rock glacier hydrology stating that these landforms act as unconfined aquifers in mountain slopes (e.g. Krainer and Mostler, 2002; Jones et al., 2019). The enrichment of solutes and trace elements in rock glacier outflows is commonly attributed to the thaw of internal ice and to the associated weathering of freshly exposed rock particles (Williams, Knauf, Caine, Liu and Verplanck et al., 2006; Ilyashuk, Ilyashuk, Psenner, Tessadri and Koinig, 2018; Colombo et al., 2018b; Munroe, 2018). Accordingly, the high values of EC, major ions, and trace elements, we observed increasing over the season, are consistent with data reported in the literature on rock glacier hydrology (e.g. Millar, Westfall and Delany 2013; Williams et al., 2006; Mair et al., 2015; Colombo et al., 2018a) and suggest that part of

the rock glacial baseflow in late-summer came from permafrost thaw, in addition to the groundwater fraction, and this increased as summer progressed. As observed in other case studies (e.g. Colombo et al., 2018a; Rotta, 2018), trace elements were found at high concentrations in rock glacial waters at Solda (As, Sr and Ba) and Zay (U, Rb), with concentrations of As (all Solda samples, up to 3-fold in September) and U (Zay, up to 3-fold in September) exceeding the EU/EPA limits for drinking water.

In stark contrast to all the patterns described above, we observed some striking differences between the two rock glacier outflows. While the Solda rock glacial stream exhibited high EC, Ca^{2+}, Mg^{2+}, SO_4^- that made this stream unique among all stations, the Zay rock glacial stream showed intermediate conditions between the Solda rock glacial and the lower kryal/glacio-rhithral stations, especially during the snowmelt period. The differences could be related in part to local topographic (channel stability) and geological features (pH and trace elements). However, we suggest that the seepage of kryal waters across the rock glacier debris, observed in the field, might play a crucial role in structuring the chemistry of rock glacial waters at Zay. In fact, turbidity and δ^2H values were consistently similar to those found in the adjacent lower kryal stations. The decreasing glacial influence from June to September was balanced by an increasing role exerted by the groundwater component and the thawing permafrost, as shown by a 3- to 4-fold increase of EC, ions and trace element concentrations. In addition, as summer progressed and the influence of glacier ablation dropped, the distinction between the two rock glacial streams became less pronounced. This provides insights on the mutual interactions between glacial and periglacial processes in deglaciating environments (see also Jones et al., 2019). In fact, rock glaciers can originate from the progressive evolution of a debris-covered glacier, under a continuum process along which the decreasing glacial influence is paralleled by increasing periglacial/permafrost conditions as deglaciation progresses (Anderson, Anderson, Armstrong, Rossi and Crump, 2018). Accordingly, the Zay rock glacial stream may represent a hydrological evidence of this glacial to periglacial transition, as the Zay rock glacier shows evidences of glacial origin from the same debris-covered glacier that feeds the Zay stream. Whatever its origin, the Solda rock glacier appears to be completely isolated from any glacial influence. Accordingly, its outflow may represent an ideal “hydrological end-member” of periglacial influence that the Zay rock glacial stream may reach in the late stages of deglaciation, when this stream becomes completely detached from the glacier imprint.

Glacial influence along the river continuum

The longitudinal surveys at Zay suggest that in the late stages of glacier retreat, under a declining and low discharge from glaciers, the paraglacial landscape exerts a strong influence on stream habitat conditions. Within this context, our new index (SGI) seems to capture the average influence of the glacier at the reach level, reflecting harsh summer conditions and a large seasonal variability of stream parameters. In turn, the IGI best reflected the diel cycles associated with the glacial influence in different periods and was a good indicator of the glacial imprint in proglacial sections. However, the collected data suggest that atmospheric conditions (e.g. solar radiation, air temperature) exerted a greater influence than the glacier over the water temperature, as values of 5-6°C were reached just 300 m below the glacier in all longitudinal survey periods. This is in line with the findings from another poorly glacierized basin in the French Pyrenees, where Khamis, Brown, Milner and Hannah (2015) found atmospheric conditions as the primary driver of the energy budgets in a glacier-fed stream during the snow-free period, under low discharges from the small glacier.

In our study, local conditions such as slope gradients seemed to override the glacier influence on channel stability in all stations below the lake, and this was reflected in the non-linear behaviour of the IGI proceeding downstream. In fact, a high glacial influence was restricted to the proglacial sections, where pronounced diel and seasonal variations of discharge, turbidity, EC, were those typical of highly glacierized areas (e.g. Milner and Petts, 1994; Milner, Brittain, Castella and Petts, 2001, Castella et al., 2001). Proglacial lakes are known to have a great buffering capacity for alpine river networks, as they can smooth water temperature variability, trap sediments, and stabilize downstream discharge (Milner and Petts, 1994, Finn et al., 2010). Also in our study, the turbid proglacial lake acted as an efficient environmental buffer and trap for suspended solids along the river continuum, as confirmed by significant reductions in IGI and SGI values below the lake compared to the inlet, in combination with decreased average values of turbidity (up to an order of magnitude) and Pfankuch index. Nevertheless, some environmental features showed unexpected patterns that cannot be explained by the presence of the lake alone. In fact, water temperature at the moraine outlet, extremely constant on a diel and daily basis, was always lower than in the lake inlet, whereas EC was higher downstream the moraine compared to upstream sites for all periods and timings. Furthermore, three surveys of the lake waters (downstream shore) at different timings during the glacier ablation survey revealed warm conditions (6.4-8.9°C) with turbidity and EC values lower but the same order of magnitude as the inflowing stream. Lower water temperatures and

higher EC values at the moraine outlet during snowmelt and glacier ablation are probably the result of processes occurring in the hypogeal flow across the moraine debris. In fact, coarse blocky deposits in alpine settings are able to buffer atmospheric temperatures in summer and to cool infiltrating warmer waters (Jones et al., 2019). In addition, proglacial moraines are generally considered as potential groundwater storage systems (Langston, Bentley, Hayashi, McClymont and Pidlisecky, 2011). Accordingly, the moraine outlet may combine the seepage of stream/lake waters with the groundwater flow, and this is corroborated by a larger groundwater component revealed by mixing models in that station compared to the upstream ones. Thus, while the turbidity drop was caused by both the lake and the moraine, the increased EC and the decreased water temperature was likely driven by the moraine baseflow.

Although not capable of cooling waters in the tributary, as found by Harrington et al. (2017) in a glacier-free catchment, the rock glacial stream does represent an important driver within the river continuum at Zay. This is demonstrated by the rise of EC below the confluence during the recession phase compared to previous periods which can be explained by the increased contribution of permafrost-influenced waters from the rock glacier. However, the decreased values of EC from the first to the second station downstream from the junction indicate an incomplete mixing of lower kryal and rock glacial waters at the upper site, which was located ca. 60 m below the confluence where the channel was very wide (20 - 30 m) and shallow (< 1 m).

The decreasing trends of turbidity below the glacial cirque reflect the linearly decreasing influence of the glacier, whereas the downstream increase of discharge and EC may reflect the increasing contribution from groundwater sources. Although some storage capacity has been reported in talus slopes (e.g. Sueker, Ryan, Kendall and Jarrett, 2000), water flow across these bodies is often rapid as these landforms typically consist of coarse blocky materials (Muir et al., 2011). In our study, similar water characteristics above and below the talus body suggest the stream water probably had a short residence time. However, minor diel fluctuations recorded for all parameters at the talus outlet compared to the upstream station are probably due to some buffering effect exerted by the talus debris, leading to relatively stable habitat conditions.

In the lower section of Zay, the observed longitudinal increase in EC values during snowmelt and glacier ablation can be explained by the contribution of krenal streams enriched in solutes, which also accounted for the lowering of turbidity and water temperature observed along the Zay stream. However, during the flow recession the EC continued to decline proceeding downstream from the glacial cirque, most likely due to the contribution from krenal tributaries being unable to

increasing EC as during the previous periods. This explanation is supported by the observed inactivity and reduced flow from several springs in this period.

The longitudinal gradients of EC recorded during the recession period, with a dominant influence from the rock glacier and negligible effect from groundwater tributaries, were also confirmed by additional longitudinal surveys (16-24/9, 4/10), and were driven by concentrations of Ca^{2+}, Mg^{2+}, SO_4^{2-}, and HCO_3^- (Supplementary A). Thus, despite the seepage of kryal waters into the debris of the active rock glacier, its outflow was capable of driving an inversion of the EC gradients along the entire Zay stream in late summer, exerting a significant influence on the stream hydrochemistry for more than 3 km downstream, until the Zay closing section. Furthermore, a previous study conducted along the main river of the Solda catchment revealed, in September, an increase of EC below the junction with the Zay Stream (Engel et al., 2019), and this suggests an even wider hydrological influence exerted by the Zay rock glacier requiring further investigation. Despite the water contribution from rock glaciers currently being considered as negligible from a catchment-scale perspective in the Alps (Krainer, Mostler and Spötl, 2007; Krainer, Chinellato, Toninandel and Lang, 2011; Geiger, Daniels, Miller and Nicholas, 2014), our results demonstrate that these landforms can have a significant role in shaping the stream habitat conditions along the Alpine river networks.

Our results provide new insights into how we sample the physical, chemical, and biological characteristics of alpine streams in the late phases of glacier retreat. In fact, the typically large diel fluctuations commonly attributed to glacier-fed systems, and driven by the cycles of glacier ablation, were only restricted to the proglacial sections. All stations below the lake showed a negligible diel variability in EC, turbidity, and discharge, and water temperature cycles were associated with the atmospheric conditions rather than the glacier ablation patterns. In contrast, rock glacial streams showed consistent physico-chemical variables, although we identified large and transient variations in water temperature and EC (increasing at ZRG, decreasing at SRG) associated with rainfall events (not shown). Thus, on the basis of the habitat parameters analysed, only krenal sites seem to be decoupled from both diel and daily patterns and from weather conditions, and a sampling strategy accounting for seasonality is important for all stream types.

CONCLUSIONS

Recent research on alpine stream ecosystems is beginning to show that the hydrological role of mountain permafrost is expected to increase as glaciers recede due to climate change (Jones et al.,

2019). Our results provide evidence to support previous findings on the hydrology and hydrochemistry of outflows from thawing rock glaciers, and clearly highlight the distinctive nature of these habitats. In fact, rock glacial streams exhibit constantly cold and clear waters, stable channels favouring the retention of organic detritus, and high concentrations of solutes and trace elements that increase over the season under the influence of thawing permafrost.

In alpine catchments with a small glacier cover, in which peak water has been surpassed, the low discharge from glaciers allows other driving forces, such as weather conditions and the contribution from non-glacial tributaries, to exert an increased hydrological influence. Within this context, the paraglacial landscape (i.e. proglacial lakes, moraines, talus bodies) and permafrost increasingly shape the habitat conditions of streams. Our research points to the importance of rock glacial streams in driving the hydrochemistry of alpine river networks, namely under permafrost thaw conditions, and for a long distance downstream.

Under continued climate change in the Alps (Gobiet et al., 2014), a sustained glacier recession in combination with a prolonged snow-free period may further boost the hydrological importance of active rock glaciers. Late summer/autumn can be considered as a “hot period” in deglaciating catchments because the combination of low discharges, a higher proportion of subglacial contribution, and the prolonged permafrost thaw cause an intense release of solutes and trace elements, with potentially significant effects on stream ecology and for drinking water quality. Given the scarce consideration dedicated so far to mountain permafrost, and its increasing hydroecological importance, we call for more research on the role of rock glaciers and the paraglacial landscape on the river continuum. As rock glacial streams have distinct habitat characteristics, increased research will provide valuable insights on their future ecological role in glacier-free alpine catchments.

SUPPLEMENTARY INFORMATION

Supplementary A. Environmental variables dataset, extensive survey analyses

Supplementary B. Trace elements dataset, extensive survey analyses

Supplementary C. Longitudinal surveys dataset

REFERENCES

Anderson, R. S., Anderson, L. S., Armstrong, W. H., Rossi, M. W., & Crump, S. E. (2018). Glaciation of alpine valleys: The glacier – debris-covered glacier – rock glacier continuum. *Geomorphology*, *311*, 127–142. DOI: 10.1016/j.geomorph.2018.03.015

Autonomous Province of Bolzano/Bozen 2018a. Historical series from the Civil Protection Agency, 1982/2012 period.

Autonomous Province of Bolzano/Bozen, 2018b. Online Geobrowser v.3. Available online at http://gis2.provinz.bz.it/geobrowser/?project=geobrowser_pro&view=geobrowser_pro_atlas-b&locale=it

Barnes, R. T., Williams, M. W., Parman, J. N., Hill, K., & Caine, N. (2014). Thawing glacial and permafrost features contribute to nitrogen export from Green Lakes Valley, Colorado Front Range, USA. *Biogeochemistry*, *117*(2–3), 413–430. DOI: 10.1007/s10533-013-9886-5

Baron, J. S., Schmidt, T. M., & Hartman M. (2009). Climate-induced changes in high elevation stream nitrate dynamics. *Global Change Biology*, *15*, 1777-1789. DOI: 10.1111/j.1365-2486.2009.01847.x

Baumgarten, B., Folie, K., & Stedingk, K. (1998). *Auf den Spuren der Knappen. Bergbau und Mineralien in Südtirol*. Tappeiner, Athesia

Beniston, M., Farinotti, D., Stoffel, M., Andreassen, L. M., Coppola, E., Eckert, N., … Vincent, C. (2018). The European mountain cryosphere: a review of its current state, trends, and future challenges. *The Cryosphere*, 12(2), 759–794. DOI: 10.5194/tc-12-759-2018

Blaen, P. J., Hannah, D. M., Brown, L. E., & Milner, A. M. (2014): Water source dynamics of high Arctic river basins. *Hydrological Processes*, *28*, 3521–3538. DOI: 10.1002/hyp.9891

Brighenti, S., Tolotti, M., Bruno, M. C., Wharton, G., Pusch, M. T., & Bertoldi, W. (2019). Ecosystem shifts in Alpine streams under glacier retreat and rock glacier thaw: a review. *Science of the Total Environment*, *675*, 542–559. DOI: 10.1016/j.scitotenv.2019.04.221

Brown, L. E., Hannah, D. M., & Milner, A. M. (2003). Alpine stream habitat classification: An alternative approach incorporating the role of dynamic water source contributions. *Arctic, Antarctic, and Alpine Research*, *35*(3), 313–322. DOI: 10.1657/1523-0430(2003)035[0313:ASHCAA]2.0.CO;2

Brown, L. E., Hannah, D. M., Milner, A. M., Soulsby, C., Hodson, A. J., & Brewer, M. J. (2006). Water source dynamics in a glacierized alpine river basin (Taillon- Gabietous, French Pyrenees). *Water Resources Research*, *42*. DOI: 10.1029/2005WR004268

Brown, L. E., Milner, A. M., & Hannah, D. M. (2010). Predicting river ecosystem response to glacial meltwater dynamics: a case study of quantitative water sourcing and glaciality index approaches. *Aquatic Sciences*, *72*(3), 325–334. DOI: 10.1007/s00027-010-0138-7

Carturan, L., Zuecco, G., Seppi, R., Zanoner, T., Borga, M., Carton, A., & Dalla Fontana, G. (2016). Catchment-Scale Permafrost Mapping using Spring Water Characteristics: Catchment-Scale Permafrost Mapping using Spring Water Characteristics. *Permafrost and Periglacial Processes*, *27*(3), 253–270. DOI: 10.1002/ppp.1875

Castella, E., Adalsteinsson, H., Brittain, J. E., Gislason, G. M., Lehmann, A., Lencioni, V., … Snook, D. L. (2001). Macrobenthic invertebrate richness and composition along a latitudinal gradient of European glacier-fed streams. *Freshwater Biology, 46*(12), 1811–1831. DOI: 10.1046/j.1365-2427.2001.00860.x

Clow, D.W., Schrott, L., Wobb, R., Campell, D.H., Torizzo, A. & Dornblaser, M. (2003). Ground water occurrence and contributions to streamflow in an alpine catchment, Colorado Front Range. *Ground Water*, *41*, 937-950. DOI: 10.1111/j.1745-6584.2003.tb02436.x

Colombo, N., Salerno, F., Gruber, S., Freppaz, M., Williams, M., Fratianni, S., & Giardino, M. (2018a). Review: Impacts of permafrost degradation on inorganic chemistry of surface fresh water. *Global and Planetary Change*, 162, 69–83. DOI: 10.1016/j.gloplacha.2017.11.017

Colombo, N., Gruber, S., Martin, M., Malandrino, M., Magnani, A., Godone, D., … Salerno, F. (2018b). Rainfall as primary driver of discharge and solute export from rock glaciers: The Col d'Olen Rock Glacier in the NW Italian Alps. *Science of the Total Environment*, *639*, 316–330. DOI: 10.1016/j.scitotenv.2018.05.098

Cuffey, K., and Paterson, W. S. B. (2019). The Physics of Glaciers (4th ed.). Elsevier Academic Press

Engel M., Penna D., Bertoldi G., Vignoli G., Tirler W., & Comiti F. (2019). Controls on spatial and temporal variability in streamflow and hydrochemistry in a glacierized catchment. *Hydrology and Earth System Sciences*, 23, 2041–2063. DOI: 10.5194/hess-23-2041-2019

Finn, D. S., Räsänen, K., & Robinson, C. T. (2010). Physical and biological changes to a lengthening stream gradient following a decade of rapid glacial recession. *Global Change Biology*, *16*(12), 3314–3326. DOI: 10.1111/j.1365-2486.2009.02160.x

Füreder, L. (1999). High alpine streams: cold habitats for insect larvae. In *Cold-adapted organisms: ecology, physiology, enzymology and molecular biology* (pp. 181–196). Berlin, Heidelberg, Germany: Springer Berlin Heidelberg

Füreder, L. (2012). Freshwater ecology: Melting biodiversity. *Nature Climate Change*, *2*(5), 318–319. DOI: 10.1038/nclimate1508

Geiger, S. T., Daniels, J. M., Miller, S. N., & Nicholas, J. W. (2014). Influence of Rock Glaciers on Stream Hydrology in the La Sal Mountains, Utah. *Arctic, Antarctic, and Alpine Research*, *46*(3), 645–658. DOI: 10.1657/1938-4246-46.3.645

Genereux D. 1998. Quantifying uncertainty in tracer-based hydrograph separations. *Water Resources Research*, *34*, 915–919. DOI: 10.1029/98WR00010

Gobiet, A., Kotlarski, S., Beniston, M., Heinrich, G., Rajczak, J., & Stoffel, M. (2014). 21st century climate change in the European Alps—A review. *Science of The Total Environment*, *493*, 1138–1151. DOI: 10.1016/j.scitotenv.2013.07.050

Gordon, N. D., MacMahon, T. A., & Finlayson, B. L. (1992). *Stream hydrology: an introduction for ecologists*. John Wiley & Sons: New York. ISBN: 978-0-470-84358-1

Haeberli, W., Schaub, Y., & Huggel, C. (2016). Increasing risks related to landslides from degrading permafrost into new lakes in de-glaciating mountain ranges. *Geomorphology*, *293*, 405-417. DOI: 10.1016/j.geomorph.2016.02.009

Hannah, D. M., Gurnell, A. M., & McGregor, G. R. (2000). Spatio – temporal variation in microclimate, the surface energy balance and ablation over a cirque glacier. *International Journal of Climatology*, *20*, 733–758. DOI: 10.1002/1097-0088(20000615)20:7<733::AID-JOC490>3.0.CO;2-F

Hannah, D. M., Brown, L. E., Milner, A. M., Gurnell, A. M., McGregor, G. R., Petts, G. E., Smith, B. P. G., & Snook, D. L. (2007). Integrating climate-hydrology-ecology for alpine river systems. *Aquatic Conservation: Marine and Freshwater Ecosystems*, *17*, 636-656. DOI: 10.1002/aqc.800

Harrington, J. S., Hayashi, M., & Kurylyk, B. L. (2017). Influence of a rock glacier spring on the stream energy budget and cold-water refuge in an alpine stream. *Hydrological Processes*, *31*(26), 4719–4733. DOI: 10.1002/hyp.11391

Harrington, J. S., Mozil, A., Hayashi, M., & Bentley, L. R. (2018). Groundwater flow and storage processes in an inactive rock glacier. *Hydrological Processes*, *32*, 3070-3088. DOI: 10.1002/hyp.13248

Hauer, F. R., & Lamberti, G. A. (1996). Methods in stream ecology. Academic Press, San Diego, CA, pp. 579- 589

Hodson, A. (2007). Phosphorus in glacial meltwaters. In *Glacier Science and Environmental Change*

(ed P. G. Knight), Blackwell Publishing, Malden, MA, USA. DOI: 10.1002/9780470750636.ch17

Huss, M., & Fischer, M. (2016). Sensitivity of Very Small Glaciers in the Swiss Alps to Future Climate Change. Frontiers in Earth Science, 4. https://doi.org/10.3389/feart.2016.00034

Huss, M., & Hock, R. (2018). Global-scale hydrological response to future glacier mass loss. Nature Climate Change, 8(2), 135–140. DOI: 10.1038/s41558-017-0049-x

Huss, M., Bookhagen, B., Huggel, C., Jacobsen, D., Bradley, R. S., Clague, J. J., … Winder, M. (2017). Toward mountains without permanent snow and ice. *Earth' s Future*, *5*, 418–435. DOI: 10.1002/ 2016EF000514

IBM (2018). SPSS Statistics software, v.26.

Ilg, C., & Castella, E. (2006). Patterns of macroinvertebrate traits along three glacial stream continuums. *Freshwater Biology*, *51*(5), 840-853. DOI: 10.1111/j.1365-2427.2006.01533.x

Ilyashuk, B.P., Ilyashuk, E.A., Psenner, R., Tessadri, R., & Koinig, K. A (2018) Rock glaciers in crystalline catchments: hidden permafrost-related threats to alpine headwater lakes. *Global Change Biology*, *24*, 1548–1562. DOI: 10.1111/gcb.13985

IAEA - International Atomic Energy Agency (2014): IAEA/GNIP precipitation sampling guide V2.02 September 2014. International Atomic Energy Agency, Vienna, Austria, pp. 19, 2014

IPCC - Intergovernmental Panel on Climate Change (2013). Climate Change 2013: The Physical Science Basis. Contribution of Working Group I to the Fifth Assessment Report of the Intergovernmental Panel on Climate Change. Stocker, T.F., D. Qin, G.-K. Plattner, M. Tignor, S.K. Allen, J. Boschung, A. Nauels, Y. Xia, V. Bex and P.M. Midgley (eds.). Cambridge, United Kingdom and New York, NY, USA: Cambridge University Press. DOI:10.1017/CBO9781107415324

Jacobsen, D., & Dangles, O. (2012). Environmental harshness and global richness patterns in glacier-fed streams. *Global Ecology and Biogeography*, *20*, 647–656. DOI: 10.1111/j.1466-8238.2011.00699.x

Jones, D. B., Harrison, S., Anderson, K., & Betts, R. A. (2018). Mountain rock glaciers contain globally significant water stores. *Scientific Reports*, 1-10. DOI: 10.1038/s41598-018-21244-w

Jones, D. B., Harrison, S., Anderson, K., & Whalley, W. B. (2019). Rock glaciers and mountain hydrology: A review. *Earth-Science Reviews*, *193*, 66-90. DOI: 10.1016/j.eartscirev.2019.04.001

Khamis, K., Brown, L. E., Milner, A. M., & Hannah, D. M. (2015). Heat exchange processes and

thermal dynamics of a glacier-fed alpine stream. *Hydrological Processes*, *29*, 3306-3317. DOI: 10.1002/hyp.10433

Khamis, K., Brown, L. E., Hannah, D. M., & Milner, A. M. (2016). Glacier – groundwater stress gradients control alpine river biodiversity. *Ecohydrology*. DOI: 10.1002/eco.1724

Krainer, K., & Mostler, W. (2002). Hydrology of active rock glaciers: examples from the Austrian Alps. *Arctic, Antarctic, and Alpine Research*, *34*(2), 142. DOI: 10.2307/1552465

Krainer, K., Mostler, W. & Spötl, C. (2007). Discharge from active rock glaciers, Austrian Alps: A stable isotope approach. *Austrian Journal of Earth Sciences*, *100*, 102–112

Krainer, K., Chinellato, G., Tonidandel, D. & Lang, K. (2011). *Analysis of the contribution of permafrost ice to the hydrological water regime*. WP7 Water resources – action 7.3 report. PermaNET project. Retrieved from http://www.permanet-alpinespace.eu/archive/pdf/WP7_3.pdf

Langston, G., Bentley, L. R., Hayashi, M., McClymont, A., & Pidlisecky, A. (2011). Internal structure and hydrological functions of an alpine proglacial moraine. *Hydrological Processes*, *25*(19), 2967-2982. DOI: 10.1002/hyp.8144

Liu, F., Williams, M. W., & Caine, N. (2004). Source waters and flow paths in an alpine catchment, Colorado Front Range, United States. *Water Resources Research*, *40*(9). DOI: 10.1029/2004WR003076

Mair, V., Lang, K., Tonindandel, D., Thaler, B., Alber, R., Lösch, B., … Tolotti, M. (2015). *Progetto Permaqua – Permafrost e il suo effetto sul bilancio idrico e sull'eologia delle acque di alta montagna*. Provincia Autonoma di Bolzano, Bolzano, Italy: Ufficio geologia e prove dei materiali.

Millar, C. I., Westfall, R. D., & Delany, D. L. (2013). Thermal and hydrologic attributes of rock glaciers and periglacial talus landforms: Sierra Nevada, California, USA. *Quaternary International*, *310*, 169–180. DOI: 10.1016/j.quaint.2012.07.019

Milner, A. M., & Petts, G. E. (1994). Glacial rivers: physical habitat and ecology. *Freshwater Biology*, *32*(2), 295–307. DOI: 10.1111/j.1365-2427.1994.tb01127.x

Milner, A.M., Brittain, J., Castella, E., & Petts, J.E. (2001). Trends of macroinvertebrates community structure in glacier-fed rivers in relation to environmental conditions: a synthesis. *Freshwater Biology*, *46*(12), 1833–1847. DOI: 10.1046/j.1365-2427.2001.00861.x.

Milner, A. M., Brown, L. E., & Hannah, D. M. (2009). Hydroecological response of river systems to shrinking glaciers. *Hydrological Processes*, *23*(1), 62–77. DOI: 10.1002/hyp.7197

Milner, A. M., Khamis, K., Battin, T J., Brittain, J. E., Barrand, N. E., Füreder, L., … Brown, L. E. (2017). Glacier shrinkage driving global changes in downstream systems. *Proceedings of the National Academy of Science*, *114*(12), 9770–9778. DOI: 10.1073/pnas.1619807114

Mitchell, A., Brown, G. H., & Fuge, R. (2001). Minor and trace element export from a glacierized Alpine headwater catchment (Haut Glacier d'Arolla, Switzerland). *Hydrological Processes*, *15*(18), 3499–3524. DOI: 10.1002/hyp.1041

Montrasio, A., Berra, F., Cariboni, M., Ceriani., M., Deichmann, N., Longhin, M., … Zappone, A. (2015). Note illustrative della Carta Geologica d'Italia, Foglio 024-Bormio. ISPRA-SGI-Regione Lombardia

Muir, D. L., Hayashi, M., & Mcclymont, A. F. (2011). Hydrological storage and transmission characteristics of an alpine talus. *Hydrological Processes*, *25*(19), 2954–2966. DOI: 10.1002/hyp.8060

Munroe, J. S. (2018). Distribution, evidence for internal ice, and possible hydrologic significance of rock glaciers in the Uinta Mountains, Utah, USA. *Quaternary Research*, *90*, 50–65. DOI: 10.1017/qua.2018.24

Pfankuch D.J. (1975) Stream Reach Inventory and Channel Stability Evaluation. US Department of Agriculture Forest Service, Region 1, Missoula, Montana, 26 pp.

Rinaldi, M., Gurnell, A. M., del Tánago, M.G., Bussettini, M., & Hendriks, D. (2016). Classification of river morphology and hydrology to support management and restoration. *Aquatic Science*, *78*, 17-33. DOI: 10.1007/s00027-015-0438-z

R Development Core Team (2017). R: a language and environment for statistical computing. R Foundation for Statistical Computing, Vienna, Austria. https://www.R-project.org/

Rogger, M., Chirico, G. B., Hausmann, H., Krainer, K., Brückl, E., Stadler, P., & Blöschl, G. (2017). Impact of mountain permafrost on flow path and runoff response in a high alpine catchment. *Water Resources Research*, *53*, 1288-1308. DOI: 10.1002/2016WR019341

Rotta, F., Cerasino, L., Occhipinti-Ambrogi, A., Rogora, M., Seppi, R., & Tolotti, M. (2018). Diatom diversity in headwaters influenced by permafrost thawing: first evidence for the Italian Alps. *Advances in Oceanography and Limnology*, *9*(2), 79-96. DOI: 10.4081/aiol.2018.7929

Sharp, M. (2006). Subglacial Drainage. In Encyclopedia of Hydrological Sciences (eds M. G. Anderson and J. J. McDonnell). DOI:10.1002/0470848944.hsa173

Smith, B. P. G., Hannah, D. M., Gurnell, A. M., & Petts, G. E. (2001). A hydrogeomorphological context for ecological research on alpine glacial rivers. *Freshwater Biology*, *46*(12), 1579–1596. DOI: 10.1046/j.1365-2427.2001.00846.x

Sueker, J. K., Ryan, J. N., Kendall C., & Jarrett R. D. (2000). Determination of hydrologic pathways during snowmelt for alpine/subalpine basins, Rocky Mountain National Park, Colorado. *Water Resources Research, 36*: 63–75. DOI: 1999WR900296

Thies, H., Nickus, U., Tolotti, M., Tessadri, R., & Krainer, K. (2013). Evidence of rock glacier melt impacts on water chemistry and diatoms in high mountain streams. *Cold Regions Science and Technology*, *96*, 77–85. DOI: 10.1016/j.coldregions.2013.06.006

Uehlinger, U., Robinson, C. T., Hieber, M., & Zah, R. (2010). The physico-chemical habitat template for periphyton in alpine glacial streams. *Hydrobiologia*, *657*, 107–121. DOI: 10.1007/s10750-009-9963-x

Wagner, T., Pauritsch, M., & Winkler, G. (2016). Impact of relict rock glaciers on spring and stream flow of alpine watersheds: Examples of the Niedere Tauern Range, Eastern Alps (Austria). *Austrian Journal of Earth Sciences*, 109(1). DOI: 10.17738/ajes.2016.0006

Ward, J. V. (1994). Ecology of alpine streams. *Freshwater Biology*, *32*(2), 277–294. DOI: 10.1111/j.1365-2427.1994.tb01126.x

Ward, J. V, Malard, F., Tockner, K., & Uehlinger, U. (1999). Influence of ground water on surface water conditions in a glacial food plain of the Swiss Alps. *Hydrological Processes*, *13*(3), 277–293. DOI: 10.1002/(SICI)1099-1085(19990228)13:3<277:AID-HYP738>3.0.CO;2-N

Weekes, A. A., Torgersen, C. E., Montgomery, D. R., Woodward, A., & Bolton, S. M. (2015). Hydrologic response to valley-scale structure in alpine headwaters. *Hydrological Processes*, *29*(3), 356–372. DOI: 10.1002/hyp.10141

WGMS - World Glacier Monitoring Service (2018). Fluctuations of glaciers browser. Powered by ESRi Suisse, Zurich, version 2.0. Available at: https://wgms.ch/fogbrowser/

Williams, M. W., Knauf, M., Caine, N., Liu, F., & Verplanck, P. L. (2006). Geochemistry and source waters of rock glacier outflow, Colorado Front Range. Permafrost and Periglacial Processes, 17(1), 13–33. DOI: 10.1002/ppp.535

Williams, M. W., Knauf, M., Cory, R., Caine, N., & Liu, F. (2007). Nitrate content and potential microbial signature of rock glacier outflow, Colorado Front Range. *Earth Surface Processes and Landforms*, *32*, 1032-1047. DOI: 10.1002/esp.1455

Winkler, G., Wagner, T., Pauritsch, M., Birk, S., Kellerer-Pirklbauer, A., Benischke, R., … Hergarten, S. (2016). Identification and assessment of groundwater flow and storage components of the relict Schöneben Rock Glacier, Niedere Tauern Range, Eastern Alps (Austria). *Hydrogeology Journal*, *24*, 937–953. DOI: 10.1007/s10040-015-1348-9

Table 1. Main features of sampling stations. Code[LS]= only longitudinal survey undertaken. Lat/Lon= coordinates referring to WGS84, UTM32N. Alt= elevation (m a.s.l.). Dist = distance from the spring (km). Slope = % average slope, obtained with clivometry maps (Autonomous Province of Bolzano/Bozen, 2018). Channel type derived from Rinaldi et al. (2016). Veg= Riparian vegetation, classes: 0=sparse/absent, 1=discontinuous alpine heat, 2= continuous alpine heat, 3= alpine heat with sparse trees and shrubs 4= canopy from trees and shrubs. Moss= abundance of mosses in the channel, classes: 0=0-5%, 1=5-10%, 2=10-30%, 3=30-50%. Different kryal habitats (i.e. upper and lower stations) are classified in this work according to the distance from the glacier snout.

Catchment	Code	Lat/Lon	Alt	Dist	Slope	Habitat type	Channel type	Veg	Moss	Bedrock[c]
Zay	Z1	625.249/ 5.156.172	2845	0	55	Upper kryal	Single-thread, straight	0	0	Orthogneiss (Quartzphyllyte)
Zay	Z2 [LS]	624.690/ 5.156.263	2811	0.13	10	Upper kryal	Double-thread	0	0	Orthogneiss
Zay	Z3	625.039/ 5.156.377	2780	0.34	18	Upper kryal	Single-thread, straight	1	0	Orthogneiss
Zay	Z4[a]	624.691/ 5.156.262	2736	0.72	10	Lower kryal	Single-thread, straight	1	3	Orthogneiss
Zay	Z5	624.278/ 5.156.281	2717	1.13	2	Lower kryal	Glacial floodplain Multi-thread	1	1	Orthogneiss
Zay	Z6 [LS]	623.870/ 5.156.156	2699	1.61	1	Lower kryal	Single-thread, sinuous	1	1	Orthogneiss
Zay	Z7	623.744/ 5.155.463	2407	2.38	4	Glacio-rhithral	Single-thread, sinuous	2	3	Orthogneiss, Flaser paragneiss
Zay	Z8 [LS]	623.696/ 5.155.423	2395	2.73	5	Glacio-rhithral	Single-thread, sinuous	2	3	Orthogneiss, Flaser paragneiss
Zay	Z9 [LS]	623.574/ 5.155.234	2350	3.04	35	Glacio-rhithral	Single-thread, sinuous	3	2	Orthogneiss, Flaser paragneiss
Zay	Z10 [LS]	623.446/ 5.155.015	2228	3.44	17	Glacio-rhithral	Single-thread, straight	3	3	Orthogneiss, Flaser paragneiss
Zay	Z11 [LS]	623.131/ 5.154.761	2148	3.8	20	Glacio-rhithral	Multi-thread	3	3	Orthogneiss, Flaser paragneiss
Zay	Z12 [LS]	622.893/ 5.154.517	2084	4.15	25	Glacio-rhithral	Multi-thread: anabranching	4	2	Orthogneiss, Flaser paragneiss
Zay	Z13[b]	622.681/ 5.154.270	1982	4.5	40	Glacio-rhithral	Single-thread, straight	4	2	Flaser paragneiss, Orthogneiss (Amphibolites)
Zay	ZRG	624.401/ 5.156.088		0	2	Rock glacial	Single-thread, sinuous	2	1	Orthogneiss
Zay	ZKN	622.936/ 5.154.442		0	22	Krenal	Single-thread, straight	4	3	Flaser paragneiss
Solda	S1	622.586/ 5.148.841	2710	0	15%	Upper Kryal	Single-thread, straight	0	0	Orthogneiss, Phyllades, Amphibolites, (Prasinites and Serpentinites)
Solda	S2	622.250/ 5.149.314	2560	0.7	10%	Upper Kryal	Multi-thread: braided	0	0	Phyllades, Amphibolites, Quartzites (Prasinites, Serpentinites)
Solda	SRG	622.737/ 5.149.517	2586	0.05	25%	Rock glacial	Single-thread, straight	2	3	Orthogneiss, Quartzphyllytes, Micaschists (Andesites)
Solda	SKN	622.298/ 5.151.224	2105	0.1	65%	Krenal	Single-thread, straight	3	2	Orthogneiss, Quartzphyllytes, Amphibolites (Dolomite)

Table 2. Results from the pairwise comparisons analyses. The values of the post-hoc test (Mann-Whitney test adjusted by the Bonferroni correction for multiple tests) are reported where differences are significant, according to the corresponding α-value and df. Stream type codes: UK= Upper Kryal, LK= Lower Kryal, GR= Glacio-rhithral, KN= Krenal, RG= Rock glacial, all= all other stream types. Month codes: JUN= June, AUG= August, SEP= September, all= all other periods. Proglacial= Z1-Z3, Others= Z4-Z13. See text for further details on measured variables.

Variable	Groups	N	p-value	Test statistic	df	Post-hoc <0.001	Post-hoc <0.01	Post-hoc <0.05
EXTENSIVE SURVEYS								
Pfankuch index	Stream type	68	<0.001	H=52.4	4	UK>GR,KN, RG		UK>LK
Turbidity	Stream type	68	<0.001	H=42.5	4	UK>KN,RG		UK>GR
Suspended Solids	Stream type	63	<0.001	H=43.6	4	UK>KN,RG	UK>GR, LK	
SiO_2	Stream type	63	<0.001	H=51.6	4	UK<RG,KN	UK<GR, LK	
Organic detritus	Stream type	67	<0.001	H=54.4	4	UK<GR,RG, KN	LK<KN	
Detritus ratio	Stream type	67	<0.001	H=43.4	4	UK<GR,KN	RG<KN	
Total P	Stream type	68	<0.001	H=25.3	4	UK>GR,KN	LK<KN	UK>RG
T_{max}	Stream type	65	<0.001	H= 32.7	4	RG<KN,GR	RG<LK	RG<UK
T_{avg}	Stream type	65	<0.001	H= 44.7	4	RG<KN,GR UK<KN,GR		
dT	Stream type	65	<0.001	H=20.4	4	RG<UK	RG<LK	RG<GR
$\delta^{18}O$	Month	67	<0.001	H=19.5	2	JUN<SEP		
$\delta^{2}H$	Month	67	<0.001	H= 20.2	2	JUN<SEP		AUG<SEP
Turbidity	Month at UK	24	0.006	H= 11.3	2		SEP<AUG	SEP<JUN
Electrical conductivity	Month at UK	24	0.003	H= 10.1	2			SEP>all
NO_3^-	Month at UK	24	<0.001	H=16.8	2	SEP<AUG		SEP>JUN
Ca^{2+}	Month at UK	24	0.005	H= 10.5	2			SEP>all
Mg^{2+}	Month at UK	24	0.031	H= 6.9	2			
SO_4^{2-}	Month at UK	24	0.011	H= 9.0	2			SEP>all
Turbidity, Pfankuch index	ZRG>SRG	12	0.002	U=36.0				
Electrical conductivity, Ca^{2+}, Mg^{2+}, SO_4^{2}, HCO_3^-, pH	SRG>ZRG	12	0.002	U=21.0				
K^+	SRG>ZRG	12	0.041	U=5.0				

Table 3. Groundwater contribution (%) resulting from the two end-member mixing analysis (groundwater versus snowmelt/ice melt, Silica concentrations as proxy). For each of the summer periods we provide the groundwater % range across the survey stations, and the mean and standard deviation values for each stream type. With the exceptions of Z1 snowmelt and Z12 (one sample), single numbers indicate the same value in both years. The relatively small values of groundwater contribution during recession are due to snow melting in the days prior to the September 2017 field campaign.

Station	Snowmelt	Ablation	Recession
S1	2.3	4.7-7.0	2.3-4.7
S2	9.3-18.6	9.3-20.9	14.0-34.9
Z1	14.0	9.3-18.6	18.6-34.9
Z3	11.6	9.3-14.0	16.3-34.9
Upper kryal	**10.0 ± 6.0**	**12.0 ± 6.1**	**20.1 ± 13.4**
Z4	46.5	41.9-48.8	30.2-62.8
Z5	39.5-41.9	39.5-44.2	30.2-62.8
Lower kryal	**42.6 ± 3.6**	**43.6 ± 4.0**	**46.5 ± 18.8**
Z7	41.9	39.5-44.2	27.9-58.1
Z12	58.1	51.2	72.1
Glacio-rhithral	**47.3 ± 9.4**	**45.0 ± 5.9**	**52.7 ± 22.6**
SKN	86.0-88.4	90.7-100.0	41.9-93.0
ZKN	88.4-93.0	97.7-100.0	46.5-93.0
Krenal	**89.0 ± 2.9**	**97.1 ± 4.4**	**68.6 ± 28.3**
SRG	46.5-51.2	58.1-69.8	27.9-58.1
ZRG	39.5-55.8	41.9-48.8	30.2-62.8
Rock glacial	**48.3 ± 6.9**	**54.7 ± 12.1**	**44.8 ± 18.3**

Table 4. Variable loadings of the environmental and trace element principal component analyses (after VariMax rotation). Bold numbers indicate strong correlation (<-0.6 or > 0.6)

	PC1	PC2
Environmental features		
PCA tot. variance	44.8%	27.9%
EC	**0.98**	0.15
SO_4^{2-}	**0.98**	0.07
Ca^{2+}	**0.98**	0.13
Mg^{2+}	**0.97**	0.08
K^+	0.35	**0.67**
Turbidity	-0.27	**-0.72**
SiO_2	0.11	**0.91**
Pfankuch	-0.11	**-0.81**
NO_3^-	0.23	0.55
T_{avg}	-0.29	**0.65**
Organic detritus	-0.08	**0.76**
Trace elements		
PCA tot. variance	41.4%	33.2%
Sr	**0.98**	0.04
Ba	**0.95**	0.05
As	**0.78**	-0.21
Rb	0.03	**0.89**
Al	-0.03	**0.85**
U	0.06	**0.71**

Table 5. Variable loadings for the Principal Component Analysis used to build the indices of Glacial Influence. Bold numbers indicate correlation > 0.6 or <-0.6

Index of Glacial Influence (IGI)[a]			**Stationary Glacier Influence (SGI)[b]**	
	PC1	PC2		PC1
1/EC	**0.91**	0.16	Turbidity SD	**1.00**
Turbidity	**0.85**	-0.20	Turbidity average	**0.99**
Pfankuch index	**0.72**	-0.55	Pfankuch index	**0.98**
1/water temperature	0.52	**0.81**	Conductivity SD	**0.86**
			1/average water temperature	**0.78**
			1/average EC	**0.70**

[a]based on single datapoints. [b]based on the whole dataset mean and SD.

FIGURE LEGENDS

Figure 1. A) Location of the study area and of the two subcatchments; B) Upper Solda; and C) Zay with location of the sampling stations and main geomorphic drivers. Station codes as in Table 1. D) Hypsographic curve of Zay stream, with indication of the monitoring stations.

Figure 2. Comparison of daily average water level (continuous line) and maximum and minimum values (dashed lines) at Z13 (2084 m a.s.l., 4.2 km far from the glacier snout) and total rainfall (columns) for both summers (until the 15th October). Gauging stations deployed on 23th June 2017. Precipitation measured at the closest meteorological station, in Solda (Autonomous Province of Bolzano/Bozen, 2018). The water stage gap in 2018 is due to a defect logging period on 9-23 June.

Figure 3. Discharge diel variability along the Zay Stream during the three longitudinal survey campaigns at different stations. Error bars indicate 95% confidence interval.

Figure 4. Mixing space of δ^2H and Silica (SiO_2) for a) Solda and b) Zay stations, including samples from potential runoff components, i.e. melting snow, supraglacial ice melt and precipitation. Different shapes indicate distinct hydrological periods: “Snowmelt”, glacier ablation (“Ablation”), flow recession (“Recession”), pooling together several sampling dates.

Figure 5. Temperature profiles for key stations in summer 2018, from the 1st of June to the 27th of September. Interruptions for the Z1 profile are caused by sensor emergence from water.

Figure 6. Boxplots of the two principal components resulting from the retained environmental variables. Boxes are clustered in terms of sampling timing, and grouped in terms of stream type except for rock glacial streams for which boxes of single stations are provided.

Figure 7. Boxplots of the two principal components resulting from the retained trace elements. Boxes are clustered in terms of sampling timing, and grouped in terms of stream type except for upper kryal and rock glacial streams, for which boxes of different catchments and single stations are provided respectively.

Figure 8. Indices of glacial influence. Seasonal Glacier Influence (SGI, black line), and the Index of Glacial Influence (IGI) boxplot for all stations and seasons. The supplementary LS campaigns were included for the calculation of the indices.

Figure 9. Longitudinal variations of the Pfankuch index (columns) and its components (lines).

Figure 10. Longitudinal patterns of the IGI, turbidity, electrical conductivity and water temperature for the three hydrological periods (snowmelt, “ablation” i.e. glacier ablation, “recession” i.e. flow recession), each calculated over all daily samplings. Mean (point) and standard deviation (area) of each sampling station and period (colours). Values for ZRG (triangles) and ZKN (circles) stations are inserted in each plot according to their position along the longitudinal gradient.

Figure 11. Timing of the minima (blue) and maxima (red) values of each variables for each hydrological period (snowmelt, “ablation” i.e. glacier ablation, “recession” i.e. flow recession), measured at 3 hours interval over 12 h. Stations and timings with constant values not represented in figures. The incomplete dataset for stations Z7/Z13 for the flow recession phase does not allow to provide results for this part of the subcatchment.

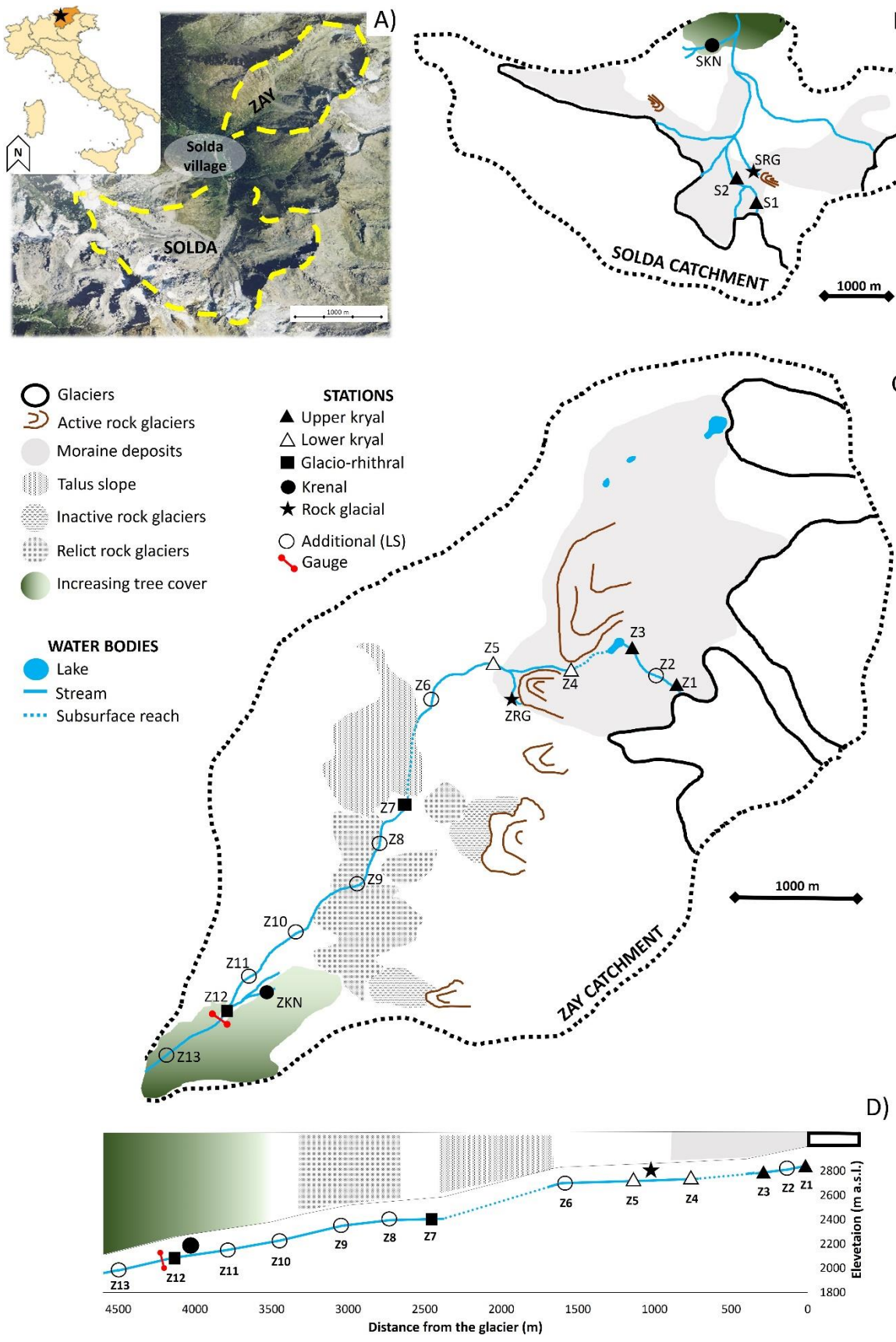
A)
ZAY
Solda village
SOLDA
1000 m
B)
SKN
SRG
S2
S1
SOLDA CATCHMENT
1000 m
C)
Glaciers
Active rock glaciers
Moraine deposits
Talus slope
Inactive rock glaciers
Relict rock glaciers
Increasing tree cover
WATER BODIES
Lake
Stream
Subsurface reach
STATIONS
Upper kryal
Lower kryal
Glacio-rhithral
Krenal
Rock glacial
Additional (LS)
Gauge
Z1
Z2
Z3
Z4
Z5
Z6
Z7
Z8
Z9
Z10
Z11
Z12
Z13
ZRG
ZKN
1000 m
ZAY CATCHMENT
D)
Elevetaion (m a.s.l.)
2800
2600
2400
2200
2000
1800
4500
4000
3500
3000
2500
2000
1500
1000
500
0
Distance from the glacier (m)

Figure 1

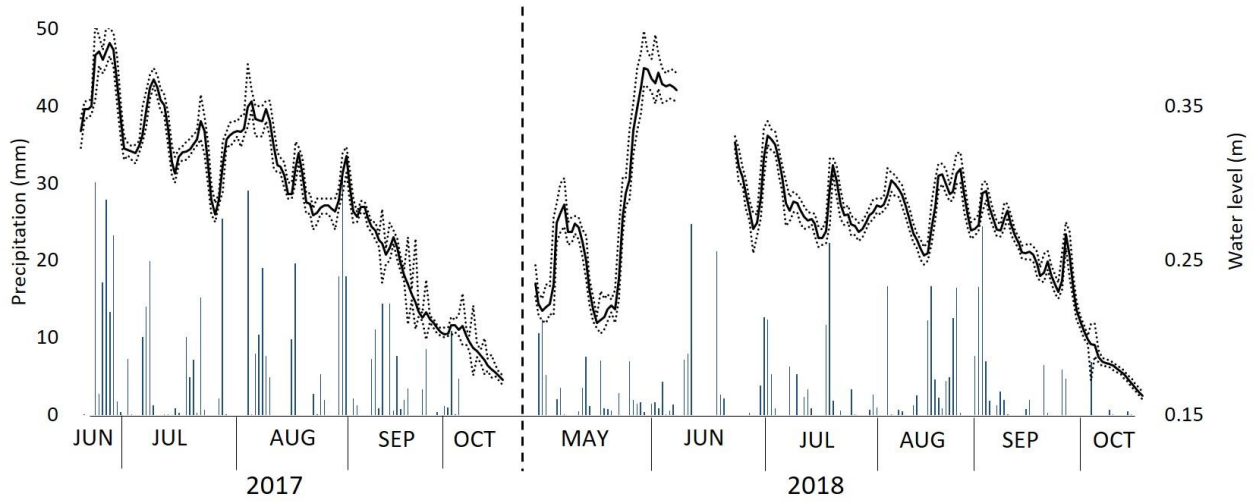

Figure 2

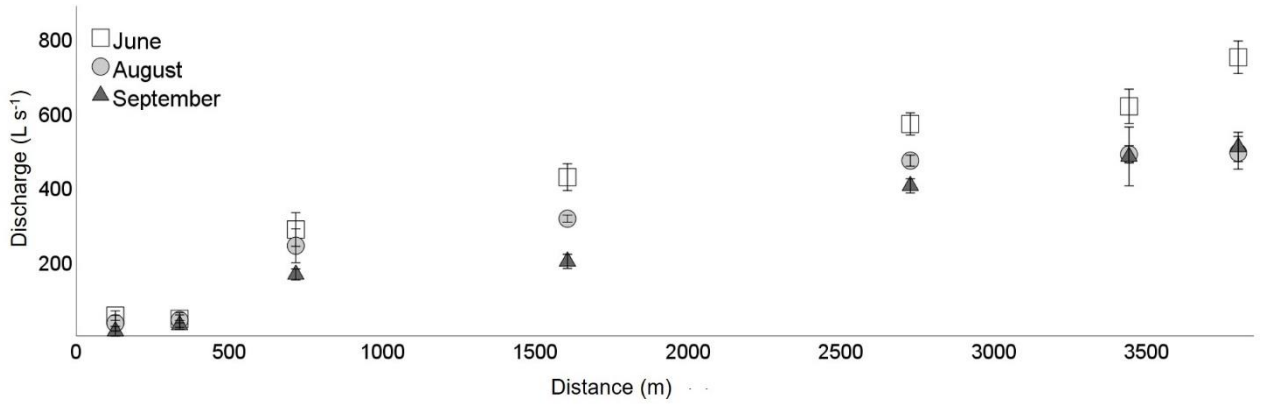

Figure 3

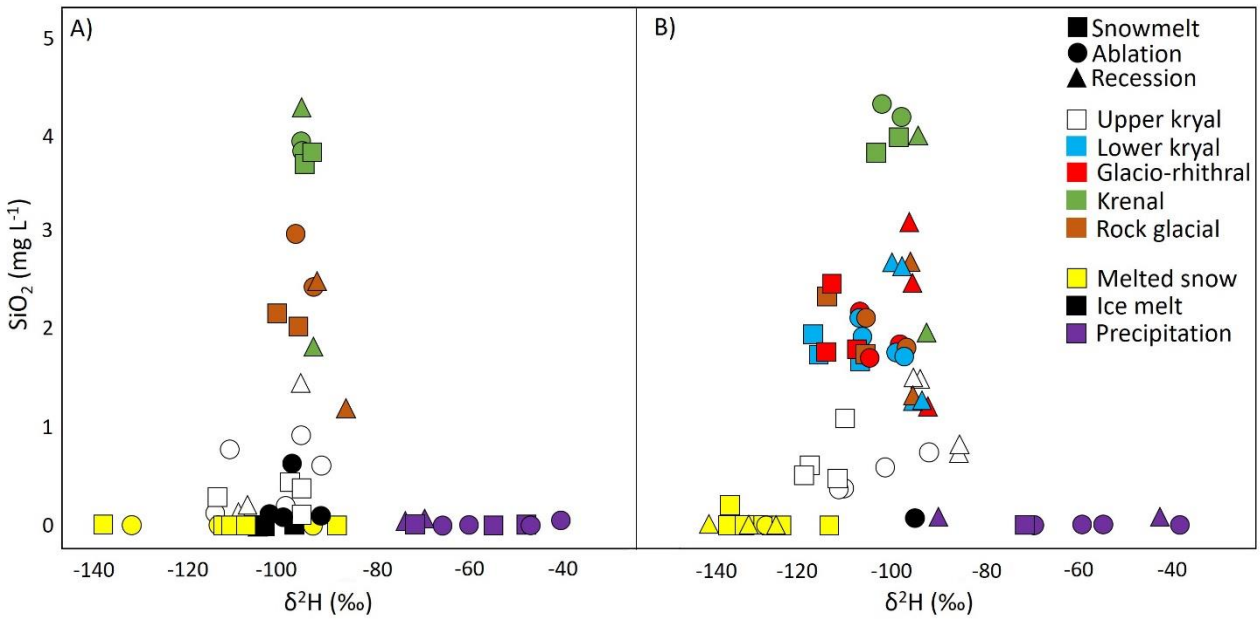

Figure 4

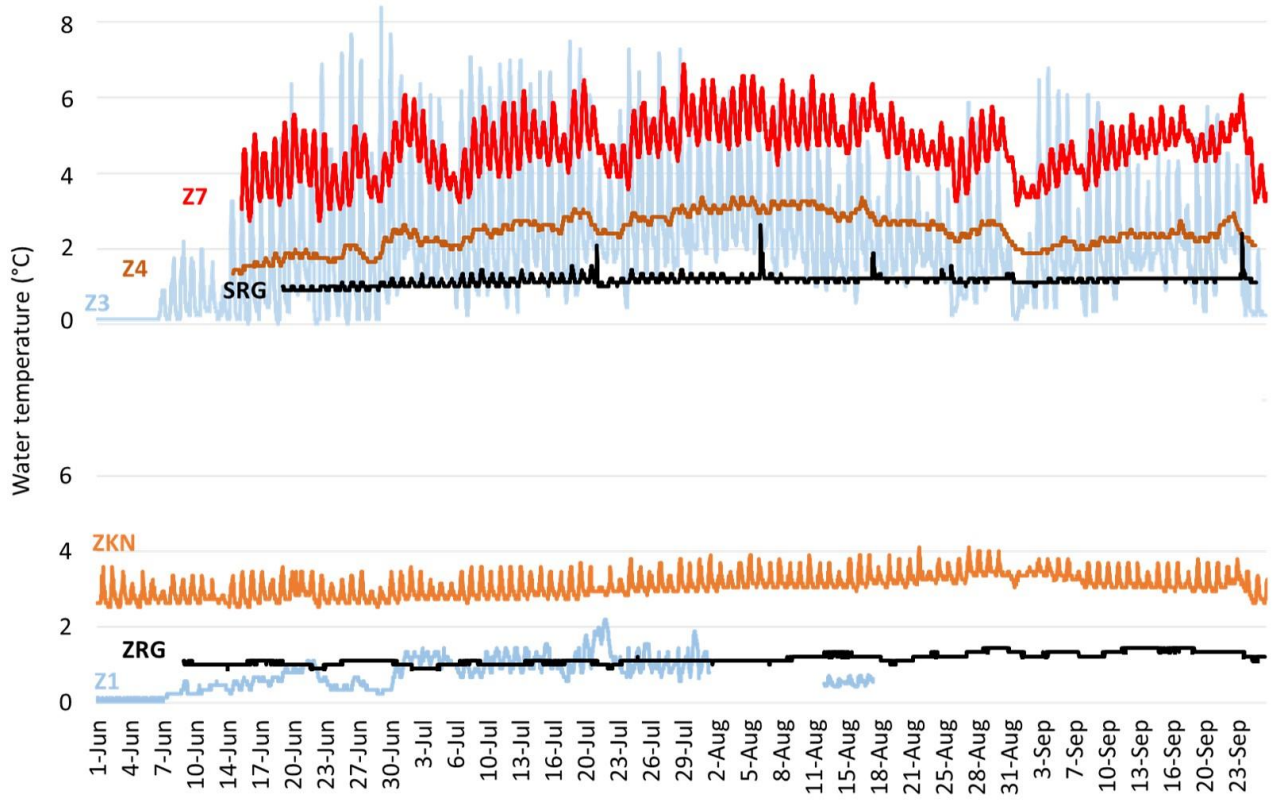

Figure 5

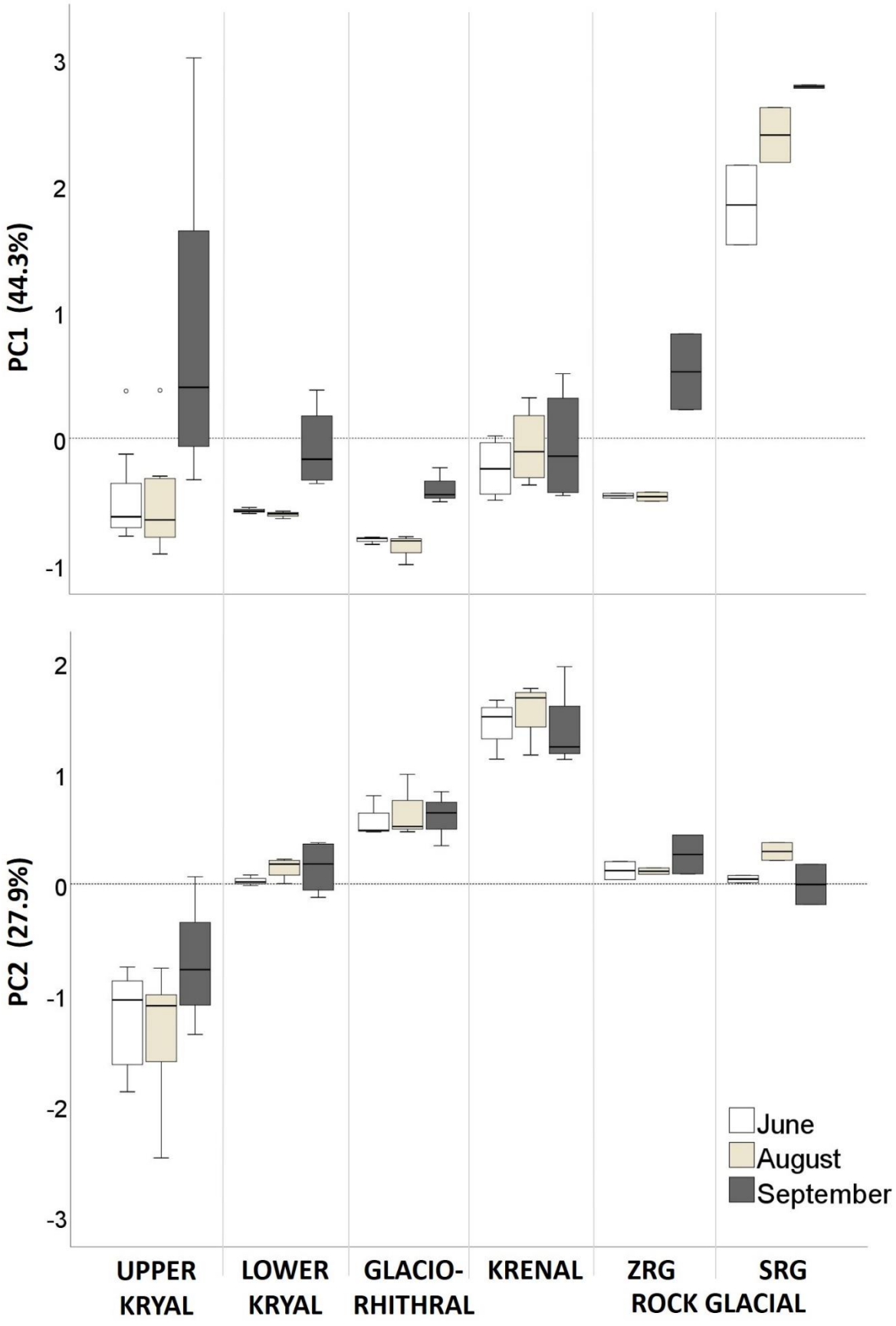
PC1 (44.3%)
3
2
1
0
-1
PC2 (27.9%)
2
1
0
-1
-2
-3
June
August
September
UPPER KRYAL
LOWER KRYAL
GLACIO-RHITHRAL
KRENAL
ZRG
SRG
ROCK GLACIAL

Figure 6

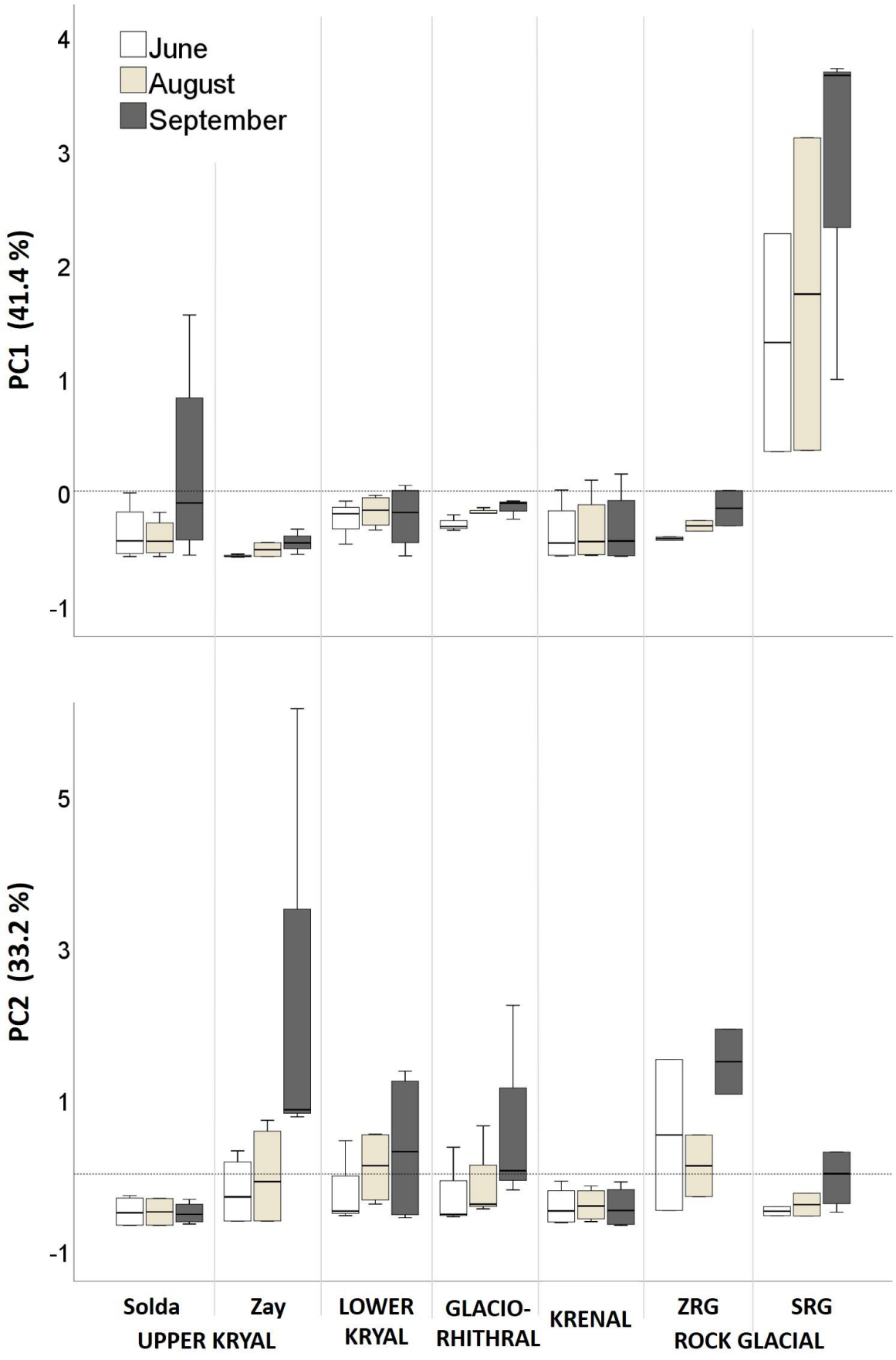
June
August
September
PC1 (41.4 %)
PC2 (33.2 %)
4
3
2
1
0
-1
5
3
1
-1
Solda
Zay
LOWER KRYAL
GLACIO-RHITHRAL
KRENAL
ZRG
SRG
UPPER KRYAL
ROCK GLACIAL

Figure 7

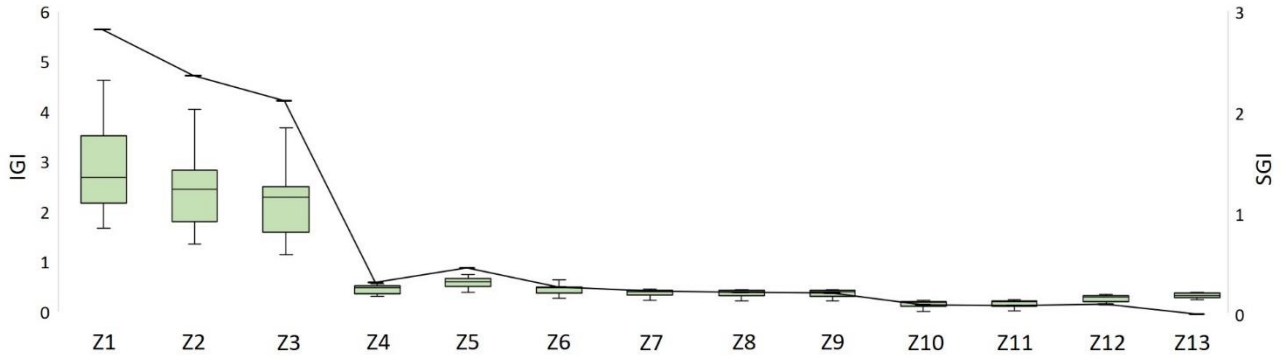

Figure 8

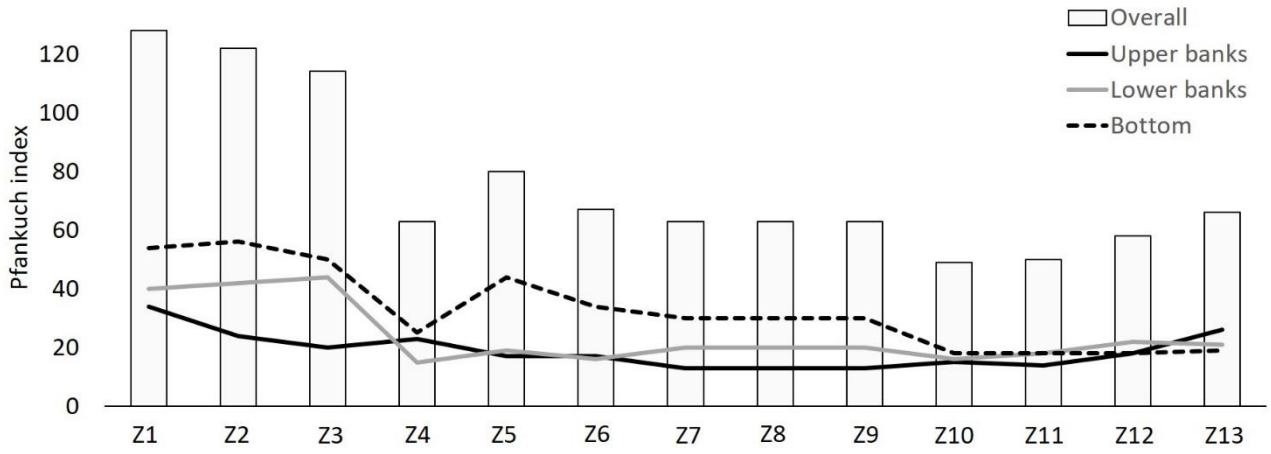

Figure 9

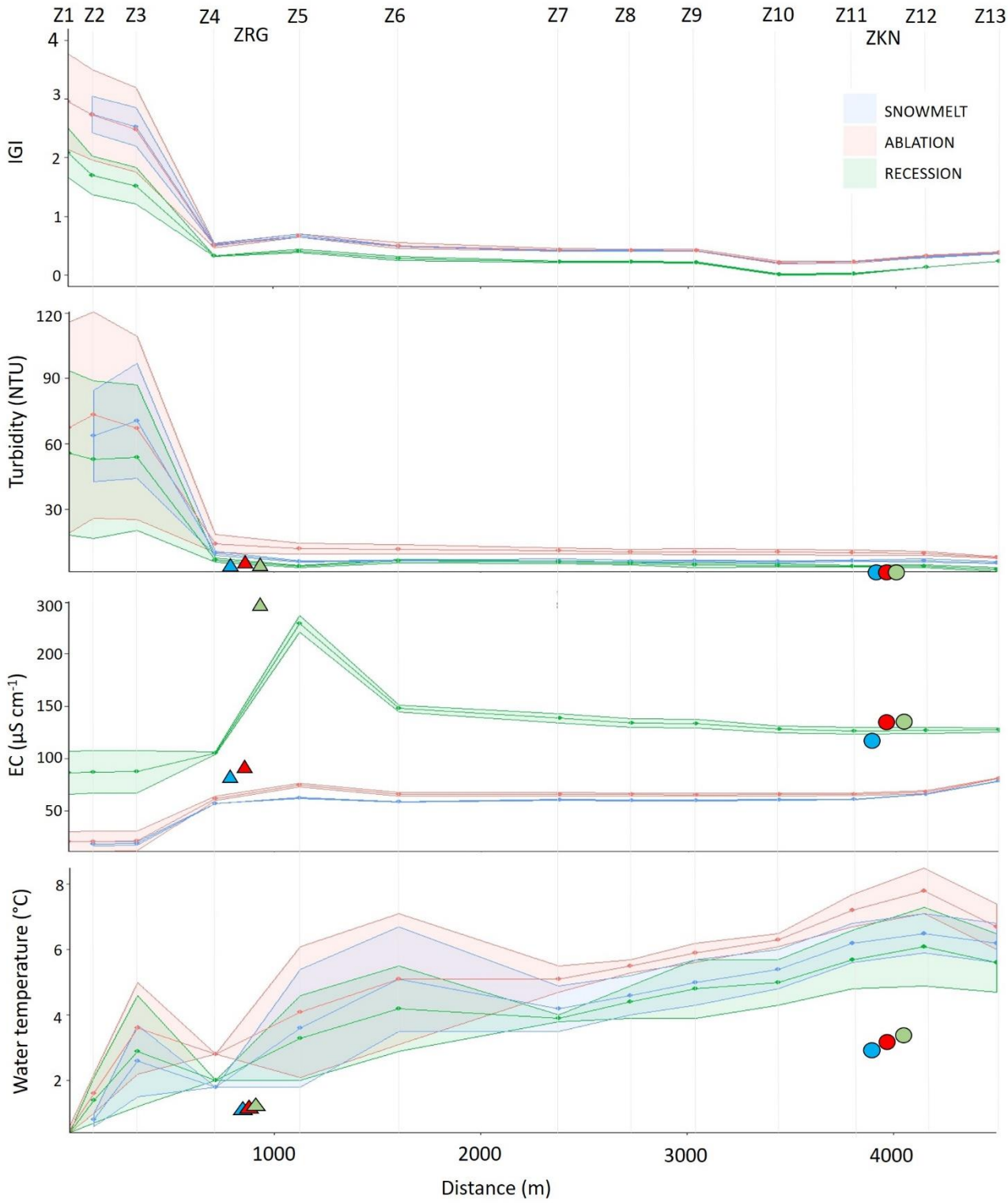
Z1
Z2
Z3
Z4
Z5
Z6
Z7
Z8
Z9
Z10
Z11
Z12
Z13
ZRG
ZKN
IGI
SNOWMELT
ABLATION
RECESSION
Turbidity (NTU)
EC (µS cm-1)
Water temperature (°C)
Distance (m)

Figure 10

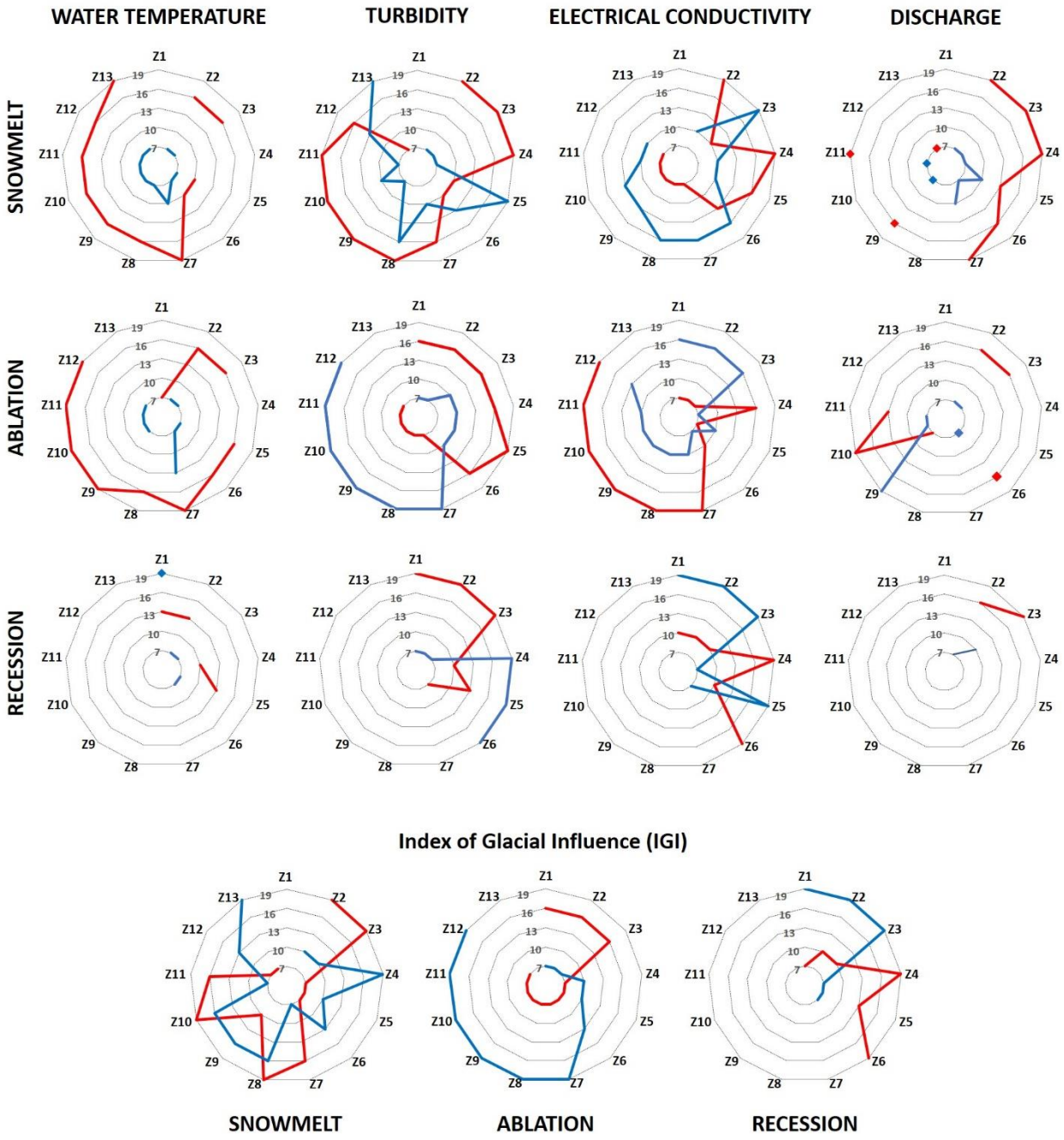
WATER TEMPERATURE
TURBIDITY
ELECTRICAL CONDUCTIVITY
DISCHARGE
SNOWMELT
ABLATION
RECESSION
Z1
Z2
Z3
Z4
Z5
Z6
Z7
Z8
Z9
Z10
Z11
Z12
Z13
19
16
13
10
7
Index of Glacial Influence (IGI)
SNOWMELT
ABLATION
RECESSION

Figure 11